MODELING PRENATAL STRESS IN HUMAN NEURAL PROGENITOR CELLS

Gayathri Ganesh

A Thesis in the Department of Neuroscience and Physiology

Submitted in partial fulfillment of the requirements for the degree of Master of Science in the College of Graduate Studies of State University of New York, Upstate Medical University.

Approved 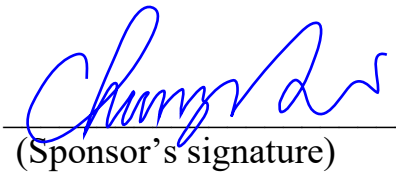
(Sponsor's signature)

Date 4-28-2023

ACKNOWLEDGEMENT

I would like to express my gratitude to Dr. Chunyu Liu, my sponsor, for his unwavering support and for providing the training environment that enabled me to successfully complete this work.

I am also grateful to my program director, Dr. Francesca Pignoni, my lab manager, Dr. Richard Kopp, and my committee members, Dr. Mariano Viapiano, Dr. Mali Wong, and Dr. Brian Howell, for their invaluable technical advice and guidance.

Additionally, I would like to acknowledge our collaborators, Chunling Zhang, for their assistance with sequencing analysis, and Dr. Michael Gandal and Dr. Dalila Pinto, for providing novel and unpublished isoform data.

I extend my thanks to the members of the graduate office, Dr. Mark Schmitt, Jennifer Brennan, Shaunna Arnold, Cherylene Small, and Jennifer Abbott, for their prompt assistance.

Finally, I am deeply grateful to my family and friends for their unconditional love and support throughout this journey.

ABSTRACT

Modeling prenatal stress in human neural progenitor cells

Author - Gayathri Ganesh

Sponsor – Dr. Chunyu Liu

Psychiatric disorders are a leading cause of disability, premature mortality, and economic burden globally, with a 48.1% increase in cases between 1990 and 2019. Stress in early life has been linked to hippocampal damage and the development of psychiatric disorders later in life. Personal stressors have also been found to be significantly associated with psychological distress, anxiety, and depression. Prenatal stress, which occurs when the fetus is exposed to excess glucocorticoids from maternal stress or synthetic glucocorticoids, has been linked to cognitive and behavioral outcomes later in life, possibly due to its impact on fetal development.

In this project, I aimed to study the effect of cortisol on neural progenitor cells (NPCs) differentiated from human induced pluripotent stem cells (iPSCs). Cell type was confirmed using iPSC and NPC marker gene and protein expression by qPCR and immunofluorescence. The loss of undifferentiation marker SSEA4 in NPCs suggests that they are differentiated. The NPCs expressed SOX2, Nestin, SOX1, and PAX6, as confirmed by qPCR and immunofluorescence analyses. The percentage of SOX2, SOX1, PAX6, and Nestin positive cells was quantified based on colocalized signals with the nuclear marker DAPI.

Novel Nestin isoforms that may be present in NPCs but not in iPSCs were identified. Currently, only one Nestin isoform is known to us. Novel, unpublished data from collaborators was used to confirm that there are Nestin isoforms present in fetal and adult human isoform sequencing study.

Glucocorticoid (GC) response genes were upregulated after cortisol treatment in NPCs, as confirmed by qPCR. I measured NPC proliferation in response to cortisol and identified that cortisol did not significantly increase NPC proliferation. However, RNA sequencing showed differential expression of proliferation-related genes in cortisol-treated NPCs. RNA sequencing analysis revealed that 59 genes were differentially expressed in cortisol treated NPCs (including

ZBTB16 and TSC22D3 measured previously using qPCR) compared to controls, out of which nine genes are associated with psychiatric traits based on GWAS studies. The study showed that cortisol can alter gene expression in NPCs, which may have implications for psychiatric disorders. Finally, the study emphasizes the novelty of exploring the role of cortisol in iPSC-derived NPCs and highlights the need for further research in this area.

TABLE OF CONTENTS

LISTING OF FIGURES

LISTING OF TABLES

ABBREVIATIONS

AD, Alzheimer's disease

ADHD, Attention deficiency and hyperactivity disorder

ASD, Autism spectrum disorder

AXD, Anxiety disorders

BD, Bipolar disorder

CRH, Corticotropin-releasing hormone.

DAPI, 4′,6-diamidino-2-phenylindole

DEX, Dexamethasone

eQTL, expression quantitative trait loci

FABP7, Fatty Acid Binding Protein 7

FOXG1, Forkhead box protein G1

GC, Glucocorticoid

GR, Glucocorticoid receptor

GW, Gestational Week

GWAS, Genome wide association studies

HPA, hypothalamic-pituitary-adrenal

iPSC, induced pluripotent stem cell.

KEGG, Kyoto Encyclopedia of Genes and Genomes

MDD, major depressive disorder

mPER, Mammalian protein extraction reagent

MR, Mineralocorticoid receptor/Mendelian randomization

mRNA, messenger RNA

NES, Nestin

NPC, Neural progenitor cell

ORF, Open Reading Frame

OTX2, Orthodenticle Homeobox 2

PAX6, Paired box 6

PBS, Phosphate Buffer Saline

PCA, Principal component analysis

POU3F2, POU Class 3 Homeobox 2

PTSD, Post traumatic stress disorder.

qPCR, quantitative polymerase chain reaction

RIN, RNA integrity number

SCZ, schizophrenia spectrum disorder

SNP, Single nucleotide polymorphism

STAR, Spliced Transcripts Alignment to a Reference

TS, Tourette syndrome.

INTRODUCTION

1.1 Psychiatric disorders

Psychiatric disorders are significant cause of years lost due to disability, premature mortality and economic burden in the society [1]. In 1990, 654.8 million cases were due to mental disorders, while this increased to 970.1 million cases in 2019. There is 48.1% increase in mental disorder cases between 1990 and 2019 [2]. People with mental disorders live with disability for many years. In 2019, 125.3 million Years lived with disability (YLDs) attributed to most of the mental disorder burden. This constitutes 14·6% of global YLDs in 2019 [2]. Mental disorders impair the function and quality of life for several decades, since many of these disorders arise in childhood, adolescence and continues throughout life, unlike many other chronic diseases [3]. The annual costs for psychiatric disorders in the US are over 200 billion USD for ADHD and ASD during early life and MDD from adolescence through midlife (Figure 1.1) [4]. At least 6 out of 8 psychiatric disorders studied are prevalent during early life, adolescence, adult and midlife (Figure 1.1) [4].

1.2 Environmental Risk of Psychiatric Disorders: Psychological Stress

There are two main paths that have been suggested by research to explain how enduring and substantial stressors experienced during adolescence can result in the development of psychosis and damage to the hippocampus later in life. The first path states that the exposure to stressors in early life is adequate to cause damage to the hippocampus. The second path proposes that genetic or gestational factors in at-risk individuals can lead to dysregulation by the prefrontal cortex of the response to stress, making the impact of less severe stressors worse [5]. Individual stressors have also been significantly and positively linked with psychological distress, anxiety, depression, and their collective profile score, mainly among females [6]. Besides, in cancer patients, psychological stress has been related to depressive and anxiety symptoms, whereas resilience was negatively associated with these symptoms [7]. Several studies on the vulnerability factors in the development of depression involved other factors such as mechanisms involved in cognitive and inflammation processing, genetic factors – gene polymorphisms and epigenetic modifiers. [8].

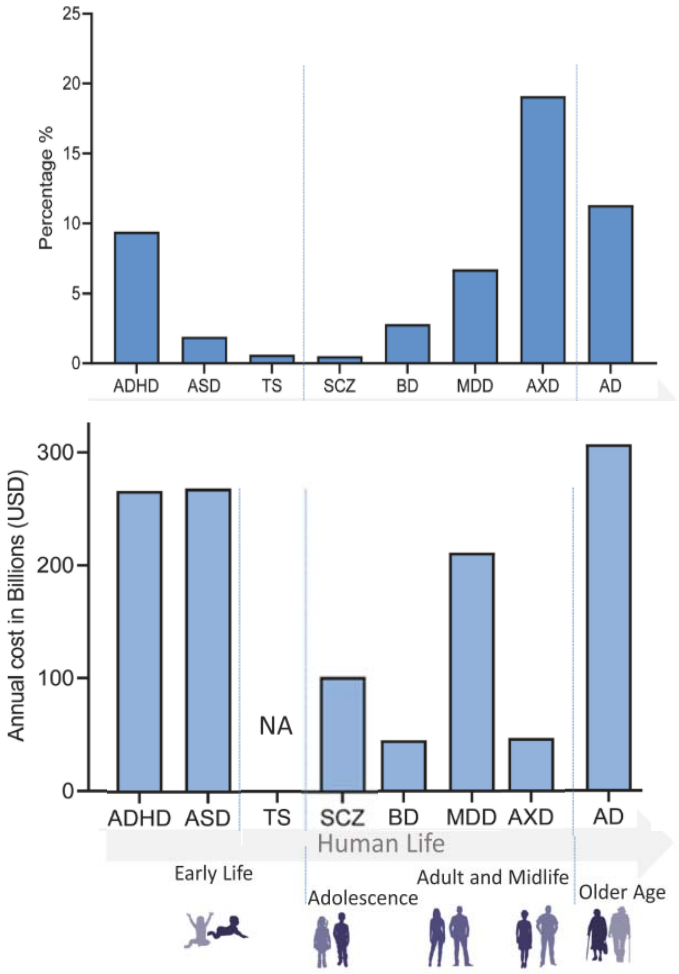

Figure 1.1: Top - The prevalence of mental disorders by age grouped based on the age of onset (percentage). Bottom - The cost of mental health disorders per year in the US (USD in billions). Results were calculated from several data sources. Figure was modified from research article [4].

1.3 Association between prenatal stress and Psychiatric disorders

1.3.1 Prenatal Stress definition, prevalence, and health impact

The investigation of mental health commonly refers to the exposure of an embryo or fetus to excessive glucocorticoids due to maternal stress as prenatal stress. Indirectly, the study of maternal stress can be conducted by observing cortisol levels, maternal depression, anxiety, PTSD, or the use of synthetic glucocorticoids.

During pregnancy, depression is prevalent in approximately 7.4% to 12.8% of cases [9], while Pregnant women face a variety of stressors such as physical, emotional, sexual abuse, or trauma, which range in prevalence from 5.3% [10] to 35% [11]. In certain cases, expectant mothers are given dexamethasone, a glucocorticoid, as a preemptive treatment for congenital adrenal hyperplasia or IVF treatment preparation. Some countries even use it to alleviate nausea during pregnancy [12-14].

The developing fetus is vulnerable to stress factors during early to mid-gestation, and prenatal stress can have a significant impact on its development [15, 16]. Cortisol, a stress hormone, can affect fetal development by crossing the placenta. The stress hormone cortisol can enter fetal circulation and affect fetal development by crossing the placenta. In fetal serum, the enzyme 11β-HSD2 typically maintains low levels of cortisol by converting cortisol into its inactive form, cortisone. However, when maternal stress levels are high, cortisol can either saturate the placental barrier or reduce levels of 11β-hydroxysteroid dehydrogenase type 2 (11β-HSD2), which allows more active cortisol to enter fetal circulation [17, 18]. Fetal development can also be affected by synthetic glucocorticoids such as dexamethasone that can penetrate the placental barrier [19]. Understanding how maternal psychosocial stress and mental health are transmitted to the fetus through the placenta is crucial to anticipate the effects of prenatal stress on the development of offspring and their outcomes in adulthood[15].

Maternal cortisol levels increase during pregnancy due to an increase in placental corticotrophin releasing hormone (CRH) production, but the placental enzyme 11β-HSD2 normally buffers fetal exposure to cortisol [15]. However, maternal psychosocial stress, depression, and anxiety can

downregulate the expression and activity of 11β-HSD2, leading to amplified maternal-fetal cortisol transfer [15].

1.3.2 Studies on correlation between maternal stress and psychiatric disorders in children

Barker's Developmental Origins of Health and Disease (DOHaD) hypothesis suggests that the origins of diseases that are non-communicable may be found during early embryonic development, a highly adaptable and vulnerable stage that is susceptible to environmental factors. The hypothesis was proposed in 1990. [16]. As an individual matures, the accumulation of diverse environmental influences coincides with decreasing biological plasticity, leading to a decreased capacity for (neuro)biological embedding of later experiences. Prenatal stress, for instance, can alter the epigenetic signature of a developing organism, resulting in long-term effects on stress reactivity and immune function. Consequently, this could increase susceptibility to psychiatric disorders later in life.

Table 1.1 – Studies on correlation between maternal stress and psychiatric disorders in children

Type of Prenatal Stress	Effect on Offspring (Increased risk for)	Statistical significance	Reference
Maternal depression	Depression	OR= 1.28; p = .003	[20]
	Depression	OR=3.4; p = 0.004	[21]
	Anxiety disorders	OR=1.75; p = 0.01	[22]
	Borderline personality disorder	OR=1.31-1.59; CI:1.14-2.32	[23]
Maternal bereavement	ADHD	HR=1.47-2.10; CI:1-3.8	[24]
	Autism & ADHD	HR=1.58; CI: 1.15–2.17, HR=1.31; CI: 1.04–1.66	[25]
Maternal cortisol levels	Affective problems	p=0.04	[26]
Maternal stressful life events	ADHD	p=0.01-0.03	[27]
	Depressive symptoms	$\beta = 0.07$, $p \leq 0.01$	[28]
	Autistic traits	$\beta = 0.16$, $p \leq 0.001$	[29]

1.4 Mechanisms of prenatal stress' impact on brain development.

1.4.1 Elevated glucocorticoid during prenatal stress and its impact on neurodevelopment, HPA axis and placenta.

Neurodevelopment

Glucocorticoids affect various tissues (brain, immune cells, muscle, fat tissues). There is a constant change in glucocorticoid and mineralocorticoid receptor expression (GR and MR) during brain development. Exposure to synthetic glucocorticoids or stressors prenatally can decrease neuronal cell proliferation, hinder neurogenesis, and modify synaptic transmission in the neocortex, dentate gyrus, and hippocampus [30, 31]. These effects are primarily mediated through the GR receptor, with vulnerable cell states being progenitor cells and adult neural stem cells expressing GR. Furthermore, glucocorticoids can influence the entire brain, resulting in reduced cortical folding, cortical thinning, altered amygdala volume, and the transmission of stress effects between generations. Research has shown that prenatal exposure to stress or glucocorticoids in animals can also cause a decrease in corpus callosum size, delayed myelination, and altered dopamine receptor binding [32, 33].

Animal Studies:

Studies conducted on animals indicate that prenatal exposure to synthetic glucocorticoids, such as dexamethasone or betamethasone, can cause a reduction in neuronal cell proliferation and alter neurogenesis in different brain regions of the offspring (neocortex, hippocampus) [30, 31]. Additionally, behavioral prenatal stressors in rodents and rhesus monkeys like maternal restraint or acoustic startle decrease volume of the hippocampus and reduce neurogenesis and the effect is mediated by the GR receptor, not the MR receptor [34, 35]. In rodents, glucocorticoid treatment and postnatal stressors can also inhibit neurogenesis and proliferation in the dentate gyrus [36].

Cellular Studies:

The use of a cell line derived from human hippocampal progenitors in in-vitro investigations has revealed that during the proliferation stage, high levels of cortisol can cause a reduction in neuronal differentiation [37]. This study highlights the heightened sensitivity of progenitor cells to elevated glucocorticoid levels, as this effect was not observed during differentiation when the cells were treated with cortisol. Furthermore, treating neuronal cultures obtained from human

induced pluripotent stem cells (iPSCs) with synthetic GR agonist dexamethasone resulted in a dose-dependent reduction in neuron count, increased proliferation of progenitor cells and astrocyte count [38, 39], further supporting the negative effects of glucocorticoids on neural development.

Glucocorticoid effects on brain regions:
GCs have significant impacts on the development and operation of the nervous system, and their effects are observed throughout the brain. Studies have shown that prenatal exposure to synthetic glucocorticoids like dexamethasone or betamethasone can lead to altered amygdala volume, cortical thinning, and reduced cortical folding in humans [40]. Moreover, maternal childhood maltreatment has been connected with decreased intracranial volume and cortical grey matter in newborns, suggesting that stress effects can be transmitted across generations [41]. In addition, maternal stress perception and depressive symptoms during pregnancy have been linked to reduced cortical thickness in childhood. This reduction is also associated with adolescent depressive symptoms [42].

HPA axis

Animal Studies:
Studies conducted on animals have revealed that the exposure to glucocorticoids during fetal development may disturb the function of fetal HPA-axis. As an example, baboons given betamethasone during the later stages of pregnancy showed a decrease in the mRNA levels of fetal pituitary gland and ACTH gene expression, as well as fetal adrenal weight at birth [43]. Dexamethasone (low dose) administration in pregnant sows heightened HPA-axis activity in their offspring, as evidenced by increased levels of ACTH and cortisol in their plasma. Sheep given high-dose dexamethasone and rats prenatally treated with dexamethasone under hypoxic conditions also exhibited similar effects [44]. These findings suggest that excessive glucocorticoid signaling during fetal development may lead to imbalanced HPA-axis activity, which has been associated with adverse neurobehavioral outcomes.

Human Studies:

The use of synthetic glucocorticoids during fetal development in human infants born at term has been linked to increased HPA-axis function and heightened cortisol responses in response to postnatal stress within the first 48 hours of life. One study found that mid-gestation exposure to betamethasone led to higher cortisol responses than exposure later in pregnancy [45]. Prenatal glucocorticoid exposure in preterm infants has been associated with decreased postnatal HPA-axis responses, although there may be confounders such as pathology during preterm births [46].

Indirect Effects:

The HPA-axis of the fetus can be indirectly influenced by prenatal stress through changes in placental function. In mice, prenatal stress during early gestation has been shown to interact with placental epigenetic status and genotype in a gender-specific way, affecting the development of the offspring's hypothalamus. Furthermore, stress in mothers during the first week of gestation has been linked to reduced O-linked-L-acetylglucosamine (OGT) levels in the placenta of male mice, which is responsible for chromatin remodeling. This alteration was associated with a decrease in body weight in the offspring and an increase in the responsiveness of the HPA-axis [47, 48].

In conclusion, both direct and indirect effects of prenatal stress on the HPA-axis have been observed in animal and human studies. These findings underscore the importance of minimizing exposure to prenatal stress and synthetic glucocorticoids to promote healthy neurodevelopment and prevent adverse neurobehavioral outcomes.

Placenta

Animal Studies:

The placenta acts as a natural barrier to protect the fetus from maternal glucocorticoids, with the help of an enzyme called 11β-hydroxysteroid dehydrogenase type 2 (11β-HSD2) that converts active cortisol to its inactive forms [49]. Recent studies showed that maternal cortisol can only reach a small portion (3%) of the fetal circulation due to the effectiveness of 11β-HSD2, and this increases to 7.3% when the enzyme is inhibited [50]. This highlights the crucial role of 11β-HSD2 in protecting the fetus. However, synthetic glucocorticoids like dexamethasone and

betamethasone can easily cross the placental barrier since they are not inactivated by 11β-HSD2, resulting in a high level of fetal exposure.

The placental barrier, which is crucial in safeguarding the fetus against maternal glucocorticoids, can be disrupted by prenatal stress through impaired placental glucocorticoid metabolism. Studies have demonstrated that prenatal stress affects placental function and may lead to increased fetal glucocorticoid levels. For instance, prenatal restraint stress during the end of pregnancy in rodents decreased glucocorticoid receptor (GR) protein levels and decreased mRNA expression of genes associated with placental function [51]. Moreover, excessive prenatal stress can potentially increase fetal cortisol levels by suppressing placental expression and activity of 11β-HSD2 [52]. Additionally, elevated glucocorticoids can impede placental vascularization, leading to insufficient placental growth and inadequate protection.

Human Studies:
The placenta plays a crucial role in fetal neurodevelopment, in addition to acting as a barrier against maternal glucocorticoids. The placenta is also important in fetal hypothalamic function and HPA-axis activity, which can be disrupted by prenatal stress leading to altered neurodevelopment. For example, a study found that highly anxious pregnant women had a strong correlation between maternal cortisol levels and amniotic fluid cortisol levels [53]. Furthermore, there is a negative between high prenatal anxiety with both the placental mRNA expression and 11β-HSD2 protein activity. Hypermethylation of the promoter region of the HSD11B2 gene (encodes the 11β-HSD2 protein), has been observed in infants with lower birth weight,, indicating a harmful intrauterine environment [54].

To summarize, the placenta acts as a natural shield against maternal glucocorticoids by utilizing 11β-HSD2. However, prenatal stress can block protective placental functions by hindering glucocorticoid metabolism and preventing placental vascularization. Furthermore, the placenta is crucial for fetal neurodevelopment and any prenatal stress can cause adverse effects on fetal hypothalamic function and HPA-axis activity.

1.4.2 Prenatal stress effects on Brain structure, function, cognition, and development.

In a review of 91 studies conducted between 2010 to 2017, it was found that prenatal stress is associated with several negative outcomes in infants, such as negative affect, internalizing and externalizing behaviors, cognitive and attention deficits, and impaired motor development. These outcomes were observed even after accounting for factors such as genotype, status (health and economic), maternal health, sex, age [55]. Furthermore, exposure to prenatal dexamethasone increases the risk of psychopathology, attention disorders, higher emotionality, internalizing behaviors, and lower sociability. Other prenatal stressors like maternal depression, cortisol levels, and prenatal dexamethasone administration have also been associated with changes in various brain areas such as the gyrus (temporal, occipital, fusiform), cortex (prefrontal and premotor), white matter tracts [56]. Nonetheless, it is important to note that prenatal stress does not always lead to adverse outcomes, and positive parental attention and tactile stimulation after birth can mitigate its negative effects [57].

1.4.3 Epigenetic reprogramming and gene expression during prenatal stress.

Challenges during prenatal development can leave long-lasting effects on cellular functions leading to systemic alterations. The way these exposures are imprinted at the molecular level is influenced by epigenetic mechanisms, such as changes to DNA methylation and modifications of histone proteins. Prenatal stress can reduce the placenta's ability to produce enzymes that modify specific histone proteins, which can have long-term effects on the offspring's behavior and endocrine response. [58]. Furthermore, the presence of elevated glucocorticoids during prenatal stage can lead to increasing glucocorticoid signaling and resulting in DNA demethylation changes in glucocorticoid response elements of certain genes. [59]. These modifications can alter the offspring's response to future stressors and impact neurodevelopmental pathways.

Studies in both animals and humans have demonstrated that prenatal stress or exposure to glucocorticoids can affect the stress response of offspring and may have transgenerational effects [60]. In human studies, epigenetic investigations have been performed in peripheral tissues, and the use of genome-wide approaches has yielded somewhat inconsistent results. The use of combined analyses with genetic and epigenetic scores may increase the ability to detect the effects of prenatal stress on the offspring's epigenome.

1.5 Experimental models to study prenatal brain development.

Several animal models have been used to study prenatal stress [61]. Studies in these models have demonstrated a role for prenatal stress in regulating neurodevelopment, HPA axis (described above), Recently, there is increased interest in developing more physiologically relevant models to investigate human prenatal stress. In this project, we use the human iPSC model to derive neural progenitors and neurons to understand the effects of cortisol on neural development.

According to several studies [62, 63], gene transcription profiles of human embryonic stem cells (hESC) and human induced pluripotent stem cells (hiPSC) derived neural progenitors and neurons resemble 16-19 week post-conception embryonic and fetal brain. Human iPSCs were differentiated to neurons and MAP2 and NeuN expression was observed in the neurons (Figure 1.2) (marker for neurons)

In vitro neuronal differentiation replicates significant neurogenic events observed in vivo, including the gradual anterior-posterior patterning. At the initial stages of differentiation, neural progenitors express anterior markers (FOXG1, PAX6, OTX2) while later progenitors express posterior markers (POU3F2, FAB7, NES) [64, 65]. Furthermore, the in vitro neuronal differentiation process mimics the formation of cortical layers in the brain. During this process, neurons located in deeper layers are produced from early progenitors, while those in more superficial layers arise from later progenitors. This is accompanied by a transition from neurogenic towards gliogenic cell fate, which is connected to changes in histone modifications and DNA methylation. As a result, the range of cell fates available to the progenitors is limited sequentially [66].

Prospective evaluation of gene x environment interactions can be carried out using induced pluripotent stem cells (hiPSC) in the laboratory, free from retrospective confounders. These stem cells provide the unique ability to investigate live human neuronal cells at different developmental stages and modify molecular mechanisms, a prospect that is unfeasible with post-mortem studies.

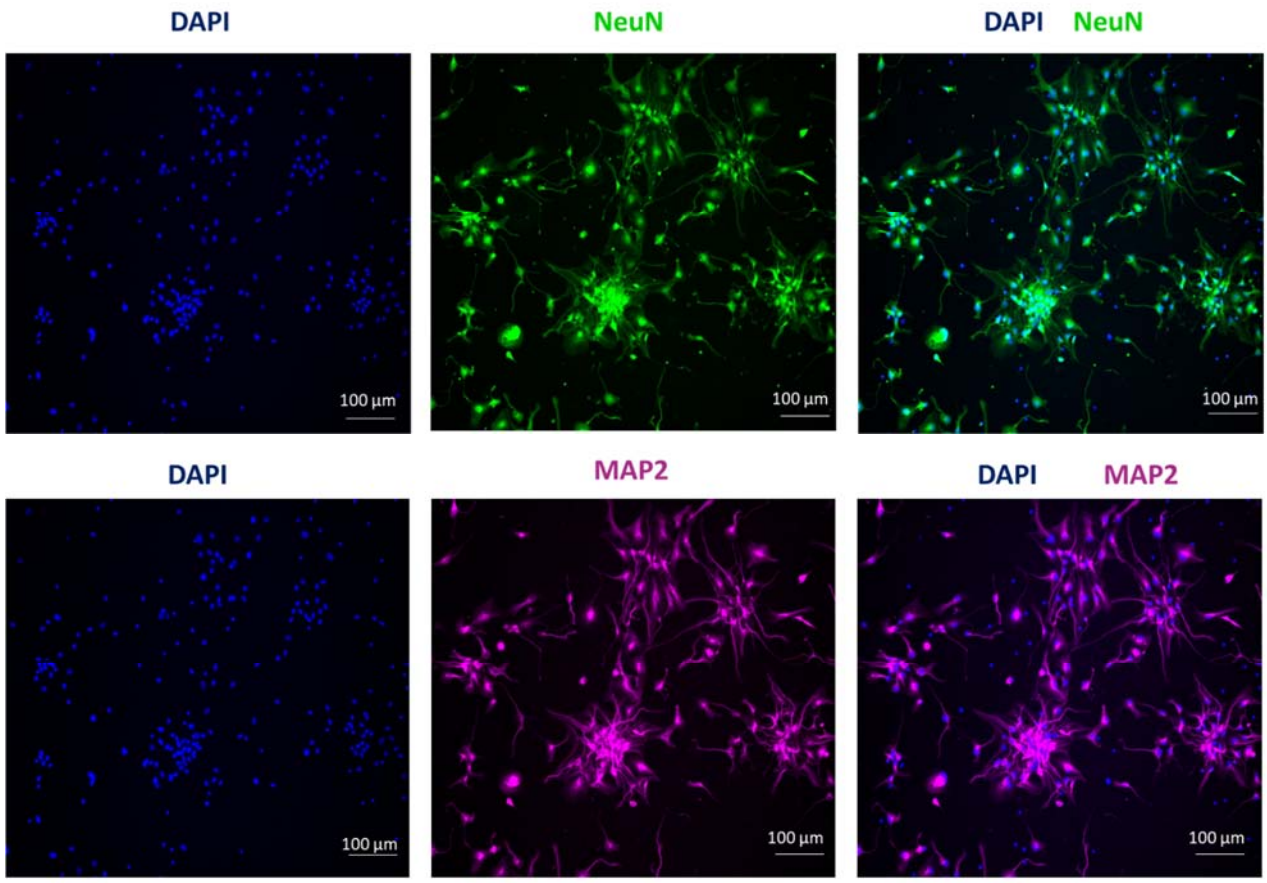

Figure 1.2: NeuN and MAP2 staining in iPSC derived Neurons.

Research Areas in the lab:

The major focus areas in this lab are:

- QTL mapping for psychiatric disorders.
- DNA methylation in psychiatric disorders.
- Comparing effects of population diversity on psychiatric disorders.
- Developing new analysis tools to identify cell types or individual samples from bulk data.

Current efforts:

Our team is dedicated to developing human cellular models of various brain cell types to investigate the effects of stress and its association with psychiatric disorders. As part of this project, I have played a pivotal role in establishing the human cellular model for studying neuron development. This involved the culturing and differentiation of human neural progenitors and neurons from iPSCs and confirming cell types using qPCR and immunofluorescence. Our collaborators in China are also working on developing glial and organoid models from human iPSCs.

Furthermore, I have conducted research on the effects of cortisol (a hormone involved in the psychological stress response) in neural progenitor cells. Through qPCR and western blotting, I have demonstrated mRNA and protein expression of cortisol response genes. I also designed and executed a pilot study to measure cortisol-related transcriptomic changes in NPCs, generating vast datasets containing valuable preliminary evidence to identify cortisol-regulated changes on the transcriptome level in different brain cell types. In this study, I prepared NPC samples for RNA sequencing and performed several downstream analyses to identify key genes associated with stress and psychiatric disorders.

Additionally, I have developed cell viability and proliferation assays to measure cortisol response in NPCs. To assess cell viability, I established MTS and Live/Dead staining methods in the lab, and optimized Ki67 and EdU-based proliferation assays to study how NPCs respond to cortisol.

In parallel, I set up the western blot system in the lab, encompassing sample preparation, protein separation, transfer, imaging, and analysis. I implemented an efficient method for protein transfer that reduces processing time by several hours. With this system, our lab can measure proteins (receptors, transcription factors, inflammatory signaling proteins, etc.) and protein modifications in response to cortisol in different brain cell types. Furthermore, this system can validate several human brain proteomic studies in cellular models.

Overall, my contributions to the development of these critical experimental tools and techniques in the lab aim to identify the role of different genes in psychiatric disorders. I hope that this work will help us develop mechanistic and validation studies in human cellular models in the future, enabling us to comprehend our findings from multi-omic studies in the human brain.

MATERIALS AND METHODS

Human iPSC Culture and maintenance

iPSC culture (details of the lines used is given in Appendix Table 3) was started from frozen stocks in Liquid nitrogen. Corning® Matrigel® Matrix solution (Cat# 354277, Corning, Corning, NY, USA) was prepared by adding 271µl to DMEM F:12 (Cat# 11320033, Thermo Fisher Scientific, Waltham, MA, USA). iPSCs suspension was thawed for few minutes at room temperature and centrifuged in 5 ml mTeSR™ Plus medium (Cat# 100-0276, STEMCELL Technologies, Vancouver, BC, Canada) at 300xg for 5 minutes. Matrigel is an extracellular matrix preparation (ECM) prepared from Engelbreth-Holm-Swarm (EHS) mouse sarcoma. Matrigel contains ECM proteins such as laminin (a major component), collagen IV, heparan sulfate proteoglycans etc. 6 ml mTeSR™ Plus was prepared with 12 µl 10mM Y-27632 (Dihydrochloride) (Cat# 72302, STEMCELL Technologies, Vancouver, BC, Canada). T25 flask was coated with 3 ml Matrigel for 1 hour at 37 C. All the cells were added to T25 flask containing 6 ml mTeSR™ Plus medium.

iPSC cells were maintained in mTeSR™ Plus medium. iPSCs were split every three-four days. For splitting, a new T25 flask was coated with matrigel and kept in incubator for atleast 1 hour. mTeSR media 6 ml + 3µl 10mM Y-27632 (Dihydrochloride) (Cat# 72302, STEMCELL Technologies, Vancouver, BC, Canada) was prepared for each T25 flask. Media was removed and cells were washed with 5 ml DPBS (Cat# 14190144, Thermo Fisher Scientific, Waltham, MA, USA). 3 ml ReLeSR (Cat#100-0484, STEMCELL Technologies, Vancouver, BC, Canada) was added to the flask and gently shaken followed by removal of ReLeSR using a glass pipette. The flask was incubated for 6 minutes. 2 ml mTESR was added using pipette on the side and mixed few times. Split ratio was calculated based on the required density followed by adding the required volume to the new flask containing 6 ml mTESR plus. Cells look like small clumps on the day of split/passage.

Quality assessment

Mycoplasma Test

Cell cultures are often contaminated with mycoplasma, with continuous cell lines being more susceptible to contamination [67]. Mycoplasma contamination alters cell morphology, metabolism, growth characteristics etc [67]. Therefore, it is important to test for mycoplasma routinely during cell culture. There are several methods to detect Mycoplasma such as ELISA, microbial growth on agar, PCR etc [67].

iPSC lines were tested for mycoplasma using Mycosensor qPCR assay (Cat# 302107-5 , Agilent Technologies, Santa Clara, CA, USA). Extracts from cell culture supernatants were prepared by boiling according to the kit protocol. To perform the procedure, 100 microliters of the supernatant from the cell culture being tested was taken and put it into a small tube for centrifugation. Then, the liquid was heated to 95°C by boiling it for 5 minutes before quickly spinning the tube for 30 to 60 seconds in a microcentrifuge. Template DNA was extracted and reagent mixture was prepared according to kit instructions. PCR reagents were provided in the kit. Sample mix (water, master mix, primer mix and reference dye) was prepared and real time PCR was done using Mx3000. PCR reaction conditions are described below. Amplification and dissociation curve plots were compared to determine Mycoplasma contamination in the sample (Figure 2.1). Results from the mycoplasma test in 2 iPSC lines are shown in Table 2.1.

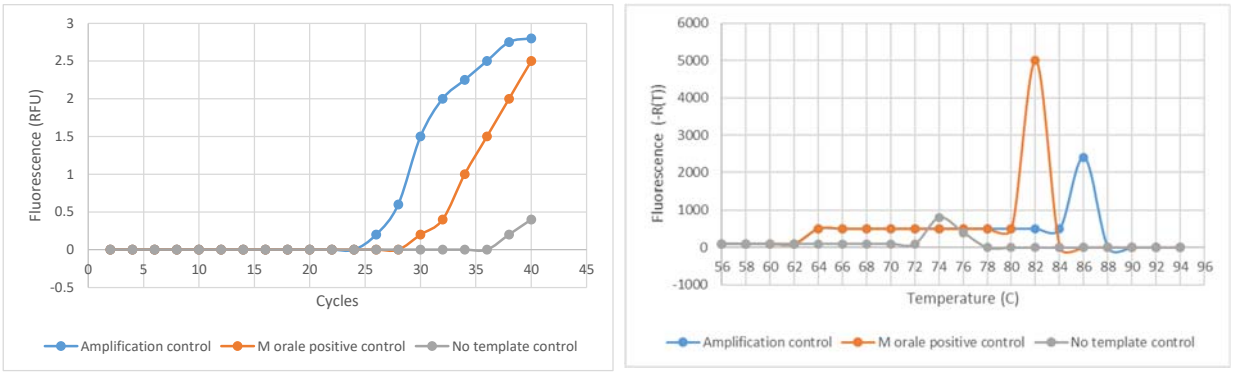

Figure 2.1: Amplification (Left) and Dissociation (Right) curve plots for reactions with and without the indicated MycoSensor kit template DNA. Mx3000P real-time PCR instrument was used to collect and analyze data. (Modified from https://www.agilent.com/cs/library/usermanuals/public/302106.pdf)

Table 2.1: Mycoplasma test results in two iPSC lines (5975 and 5983)

	Samples (S – supernatant, C-cell lysate, NTC – no template control.)	Amplification Duplicate 1	Amplification Duplicate 2	Melting Temp 1	Melting Temp 2
1.	M. orale positive control	Yes	Yes	80.4 °C	83.9 °C
2.	M. orale positive control	Yes	No	80.9 °C	79.4 °C
3.	Amplification Control	Yes	Yes	83.9 °C	83.9 °C
4.	NTC	No	No	76.8 °C	76.8 °C
5.	5975 C	No	No	75.2 °C	75.2 °C
6.	5975C + Amplification Control	Yes	Yes	83.8 °C	83.8 °C
7.	5975 S	No	Yes (Ct 31.65)	80.3 °C	75.2 °C

8.	5975S + Amplification Control	Yes	Yes	84.4 °C	80.3 °C
9.	5983 C	Yes (No Ct)	No	78.4 °C	80.8 °C
10.	5983 C + Amplification Control	Yes	Yes	83.9 °C	83.8 °C
11.	5983 S	No	No	85.4 °C	83.3 °C
12.	5983S + AmpC	Yes	Yes	83.8 °C	83.9 °C

iPSC-NPC differentiation

6 well plates were coated with Corning® Matrigel® for 1 hour at 37 C. STEMdiff™ Neural Induction Medium + SMADi (Cat# 08581, STEMCELL Technologies, Vancouver, BC, Canada) + 10 µM Y-27632 was prepared and warmed at 37°C). iPSCs were washed once with 5 mL sterile PBS and 3 mL Accutase was added to the T25 flask and kept at 37 C for 6 minutes. The cell suspension was mixed up and down 3 - 5 times using a pipettor to make single cell suspension. Using a 5 mL serological pipette, the cells were transferred into a 15 mL conical tube containing 5 mL of DMEM F12 that was supplemented with 15mM HEPES. This mixture was centrifuged at a speed of 300 x g for a period of 5 to 10 minutes, after which the supernatant was gently removed, and the cells were suspended in STEMdiff™ Neural Induction Medium, along with SMADi and 10 µM Y-27632. The final concentration of cells was adjusted to 1 x 10^6 cells/mL (equivalent to 2 x 10^5 cells/cm2). Cell counting was carried out using Countess 3FL (Thermo Fisher Scientific, Waltham, MA, USA) by diluting the cells in Trypan Blue at a ratio of 1:1. The Matrigel was removed from the 6-well plate, and cells were placed in the plate

at a recommended density range of 2 to 2.5 x 10^5 cells/cm2. A total of 2 mL of the cell suspension (containing 2 x 10^6 cells/well) was added to a single well of the Matrigel-coated 6-well plate. Daily full medium change was done using STEMdiff™ Neural Induction Medium + SMADi or until cultures are ready for passage.

Passaging cells for iPSC-NPC differentiation

NPCs are passaged between Day 6 – 9 based on cell growth rate. 6 well plate was coated with Corning® Matrigel®. Medium was aspirated from NPC containing well and 1 mL of ACCUTASE was added to the wells and kept at 37°C for 5 - 10 minutes. To detach any remaining cells, the cell suspension was thoroughly mixed using a pipettor. Following this, 5 mL of DMEM/F-12 was added to the well, and the NPC suspension was transferred to a 15 mL conical tube before centrifugation at a speed of 300 x g for 5 minutes. The supernatant was carefully removed, and 1 mL of complete STEMdiff™ Neural Induction Medium + SMADi was added to the tube and mixed well using a pipettor. The cells were diluted in Trypan Blue at a ratio of 1:1 and counted using Countess 3FL. The Matrigel solution was removed from the new 6-well plate, and cells were placed in the plate at a recommended density range of 1.5 to 2 x 10^5 cells/cm2, with 2 mL of STEMdiff™ Neural Induction Medium + SMADi added to a single well. Plates were kept in a 37°C incubator. Medium was changed daily using STEMdiff™ Neural Induction Medium + SMADi. The timing of the next passage was determined by checking cell growth and morphology. NPCs are passaged according to the monolayer protocol (Figure 2.2).

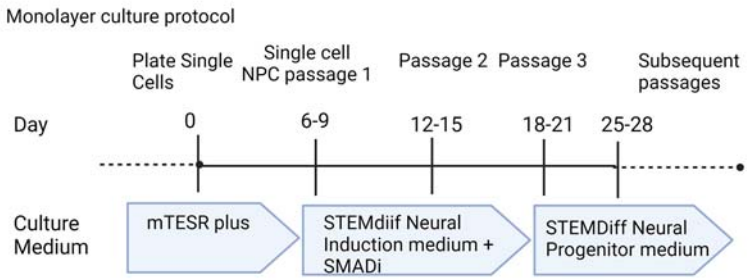

Figure 2.2: NPC differentiation protocol
(Modified from https://cdn.stemcell.com/media/files/manual/10000005588-Generation_Neural_Progenitor_Cells_from_hPSCs_using_STEMdiff_Neural_Induction_Medium.pdf?_ga=2.198277676.2019000258.1681156913-1367012267.1681156913)

using the same protocol as described above in the iPSC-NPC passaging section, with the only difference being that STEMdiff™ Neural Progenitor Medium was used instead of STEMdiff™ Neural Induction Medium + SMADi. The NPCs were then maintained in complete STEMdiff™ Neural Progenitor Medium, which is created by mixing Basal Medium [05834], Supplement A [05836], and Supplement B [05837]. Medium was changed daily.

Cryopreservation of NPCs

Single-cell suspension of NPCs were prepared using the protocol for Passaging cells for iPSC-NPC differentiation (described above). Cells were centrifuged at 300 x g for 5 minutes. Cells were diluted in 1:1 Trypan Blue and counted using automated cell counter Countess 3FL. The supernatant was removed, and the pellet itself was mixed with cold (2-8°C) STEMdiff™ Neural Progenitor Freezing Medium to create a suspension of 2-4 x 10^6 cells per milliliter. One milliliter of the cell suspension was then added to each cryovial, and the vials were placed in liquid nitrogen at a temperature of -135°C for freezing.

Thawing NPCs

6-well tissue culture plate was treated with Corning® Matrigel® (1mL per well). Cells were thawed quickly in 37°C water bath. The cells were transferred from the cryovial to the tube containing 10 mL DMEM/F-12. Cells were centrifuged at 300 x g for 5 minutes. Medium was

aspirated and the cell pellet was resuspended in 2 mL of STEMdiff™ Neural Progenitor Medium. Matrigel was removed from the 6 well plate and cell were added to a single well. The plate was kept in a 37°C incubator.

NPC-Neuron Differentiation

PLO solution was prepared in phosphate-buffered saline (PBS). 2 mL PLO solution was added to one well of 6 well plate and sealed with Parafilm® and kept overnight at 4°C. A solution containing laminin with a concentration of 5 µg/mL was diluted in DMEM/F-12. The plate that had been coated with PLO was washed twice using PBS (sterile). PBS was aspirated from the plate and 2 mL laminin solution was added and kept for 2 hours at 37 C. STEMdiff™ Forebrain Neuron Differentiation Medium (Cat# 08600, STEMCELL Technologies, Vancouver, BC, Canada) was prepared according to the kit instructions. Around Day 18 - 21 (Passage 3) (as shown in Figure) , cells were passaged according to the protocol for passaging (described above). To start the experiment, single cells were placed into a well of a 6-well plate that had been coated with PLO and laminin. The density of the cells added was between 80 and 125,000 cells per square centimeter. The cells were then transferred to 2 mL of STEMdiff™ Neural Induction Medium + SMADi. After a period of 24 hours, the medium was removed and replaced with 2 mL of STEMdiff™ Forebrain Neuron Differentiation Medium. The cells were then placed in an incubator at 37°C and 5% CO2. Medium was changed daily till cells reached 80-90% confluency (around day 25-28). The Stemdiff™ Forebrain Neuron Maturation Medium, which includes BrainPhys™ Neuronal Medium and Maturation Supplement, was made following the guidelines provided in the kit. To prepare the plates for the experiment, 6-well plates coated with PLO and laminin were used. Next, 1 mL of ACCUTASE™ was added to the neuronal precursors, which were then left at a temperature of 37°C for 5-10 minutes. Subsequently, 5 mL of DMEM/F-12 was added to the wells, and the cells were collected in a 15mL tube and centrifuged at a rate of 400 x g for a duration of 5 minutes. The supernatant was removed and cells were resuspended in 2 mL STEMdiff™ Forebrain Neuron Maturation Medium. Cells were diluted in 1:1 Trypan Blue and counted using automated cell counter Countess 3FL. Neuronal precursors were placed onto cultureware that had been coated with PLO and laminin. The cells were added at a concentration between 40000 to 60000 cells per square centimeter in 2 mL STEMdiff™ Forebrain Neuron Maturation Medium. Medium was changed every 2-3 days.

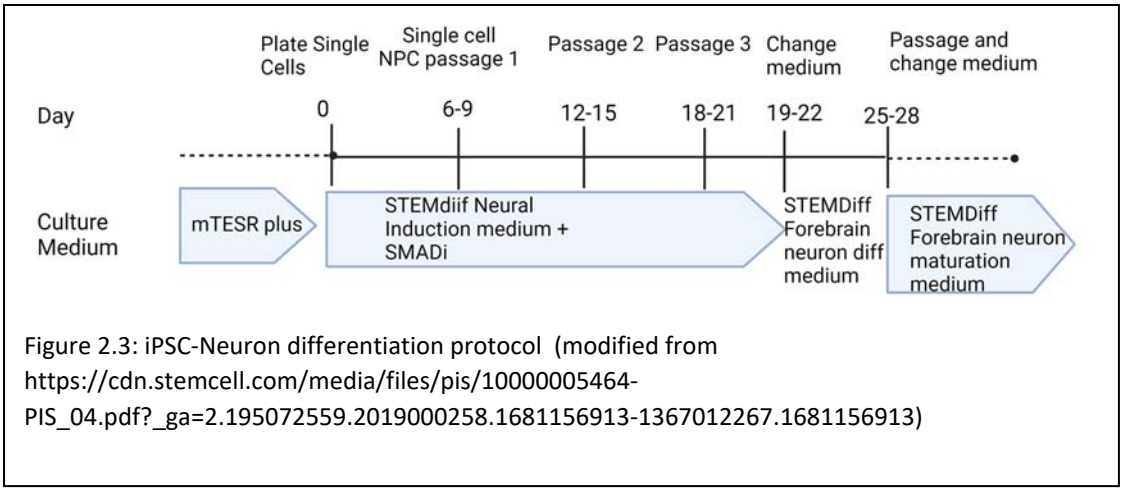

Figure 2.3: iPSC-Neuron differentiation protocol (modified from https://cdn.stemcell.com/media/files/pis/10000005464-PIS_04.pdf?_ga=2.195072559.2019000258.1681156913-1367012267.1681156913)

Microscopy

Live imaging of Neuron differentiation

Neurons were labeled with 0.25uM NeuO (Cat # 01801, StemCell Technologies, Vancouver, BC, Canada) dye in 1ml Stem diff forebrain neuron maturation media, and incubated for 1 hour at 37 C. Media was removed and replaced with fresh 2 mL

Stem diff forebrain neuron maturation media. Images were taken using Zeiss Axiovert CFL 40.

Immunofluorescence

Coverslips (Cat# 801011, Wuxi NEST Biotechnology, Jiangsu, China) were sterilized in 70% ethanol and placed in 6 well plates. Plates with coverslips were coated with 2 ml Matrigel for 1 hour at 37 C. Matrigel was aspirated and 200,00 cells were seeded in 2 ml appropriate media for the cells and left overnight in the CO2 incubator.

Next day, cells were fixed with 4% Paraformaldehyde for 10 min at room temperature and washed 3 times with 1 ml of 1X PBS. 1 ml of 0.1% Triton X-100 in 1X PBS was added to the cells for permeabilization for 15 min at room temperature, removed and washed three times with 1 ml of 1X PBS. 2 ml of 2% BSA in 1X PBS was added for blocking at room temperature for 60 min. The desired concentration of primary antibody diluted in 1.5 ml of 2 % BSA was added to the cells. Antibodies and concentrations used are listed in the Appendix. The plates were sealed with Parafilm and incubated overnight at 4°C. Next Day, primary antibody solution was removed

and cells were washed three times with 1 ml of 1X PBS. The desired concentration of fluorescent dye–labeled secondary antibody along with DAPI (Cat# 62248, Thermo Fisher, Waltham, MA, USA) (0.1µg/ml) diluted in 2 ml of 2% BSA was added to cells and kept in the dark for 45 min at room temperature. Cells were washed three times with 1 ml of 1X PBS. A drop of Hydromount (Cat#NAT1324, National Diagnostics, Atlanta, GA, USA) was added to each glass slide (Cat# 12-550-15, Fisher Scientific, Waltham, MA). Coverslips were gently removed from 6 well plates using forceps and placed on the glass slides.

Images were acquired using Nikon Eclipse Ti inverted microscope using 20X objective and DAPI, GFP, TRITC and Cy5 fluorescent channels. Three images per replicate were taken for SOX2, Nestin, PAX6, SOX1, MAP2 and NeuN stained cells and Five representative images per replicate were captured for Ki67 stained cells. DAPI stained images were included for all replicates and images. Exposure settings were optimized for all channels in the NIS elements software with DAPI exposure 100ms, GFP 100ms, Cy5 50ms, TRITC 300ms.

Image Analysis

Images were analyzed using ImageJ 1.53t. DAPI Images were converted to 8 bit, followed by adjusting the threshold. SOX2/SOX1/PAX6/Ki67 images were also converted to 8 bit and threshold adjusted. DAPI colocalization images were made using AND function in Image calculator. Cells were counted in DAPI and DAPI+SOX2/SOX1/PAX6/Ki67 images using Analyze particles function. Cell counts were analyzed and bar graphs were created using GraphPad Prism 9.5.0.730.

Cortisol Treatment

Physiologically relevant cortisol concentrations were determined from previous studies on cortisol measurements in placenta and serum[26, 68]. Hydrocortisone was purchased from Millipore Sigma (Cat# H0888, Millipore Sigma, Burlington, MA, USA). Hydrocortisone has a molecular weight of 362.46 g/mol. Stock solution of 55.24mM was prepared in DMSO. Working solutions of 1mM (Add 1µl stock solution to 54µl media) and 0.1mM solution (1µl stock solution to 551µl media) were prepared. The following dilutions were used for NPC treatments:

0.5µM - 10µl from 0.1mM solution was added to 2ml NPC media in culture

1µM - 2µl from 1mM solution was added to 2ml NPC media in culture

3µM - 6µl from 1mM solution was added to 2ml NPC media in culture

Dexamethasone Treatment

Dexamethasone was purchased from Fisher Scientific (Cat# A1759003, Fisher Scientific, Waltham, MA, USA). Dexamethasone has a molecular weight of 392.464 g/mol. Stock solution 25mg/ml (63mM) was prepared in DMSO. Working solution of 0.1mM was prepared by adding 1µl stock solution in 629µl NPC medium for 0.1mM solution. For 100nM concentration used in experiments 2µl of 0.1mM solution was added to 2 ml media in culture.

Cell Viability

MTS Assay

30,000 NPCs were seeded in Matrigel coated 24 well plate 250µL STEMdiff™ Neural Progenitor Medium . DMSO or cortisol was added to the cells and kept in the incubator at 37 C for 24 hours. 50µL of CellTiter 96® AQueous One Solution Reagent (Cat# G3582, Promega, Madison, WI, USA) was added into each well of the 24 well plate. The plate was incubated at 37°C for 2 hours. Absorbance was recorded at 490nm and 700nm using Synergy H1 plate reader.

Data Analysis

Data was acquired in Gen5 3.08 software and analyzed using Microsoft Excel. Absorbance of the blank wells were subtracted from all the wells followed by subtraction of the absorbance at 700nm. Absorbance of treated cells were divided by the average absorbance emitted from the cells in the control wells. This ratio of dead cells to living cell was multiplied by 100 to give cell viability in %. Graphs were made using GraphPad Prism 9.5.0.730.

Fluorescence based viability assay.

200,000 NPCs were seeded in Matrigel coated 6 well plate. DMSO or cortisol was added to the cells and kept in the incubator at 37 C for 24 hours. Medium was collected in a 15 mL tube and 1 mL of ACCUTASE was added to the wells and kept at 37°C for 5 - 10 minutes. 5 mL of DMEM/F-12 was added to the well and NPC suspension was transferred to the 15 mL conical tube followed by centrifugation at 300 x g for 5 minutes. The supernatant was aspirated and 1 mL of complete STEMdiff™ Neural Induction Medium + SMADi was added to the tube and mixed well with pipettor.

Cell viability was determined using LIVE/DEAD™ Viability/Cytotoxicity Kit, for mammalian cells (Cat# L3224, Thermo Fisher, Waltham, MA, USA). 4 µM EthD-1 solution was made by adding 2µL of the supplied 2 mM Ethidium Homodimer-1 to 1 mL of D-PBS. 0.5 µL of 4 mM calcein AM stock solution was added to the 1 mL EthD-1 solution. The resulting solution was vortexed to ensure thorough mixing. 100µL cells were diluted in 100µL Live/Dead dye solution. Cells were counted using Countess 3FL (Thermo Fisher, Waltham, MA, USA).Graphs of cell counts were made using GraphPad Prism 9.5.0.730.

Cell Proliferation

EdU staining

Coverslips (Cat# 801011, Wuxi NEST Biotechnology, Jiangsu, China) were sterilized in 70% ethanol and placed in 6 well plates. Plates with coverslips were coated with 2 ml Matrigel for 1 hour at 37 °C. Matrigel was aspirated and 200,000 cells were seeded in 2 ml appropriate media for the cells and left overnight in the CO2 incubator. Cell proliferation was determined using Click-iT™ EdU Cell Proliferation Kit for Imaging, Alexa Fluor™ 488 dye (Cat# C10337, Thermo Fisher, Waltham, MA, USA). Half media was removed, EdU was added at a final concentration of 10 µM. EdU was prepared according to the kit instructions.

Cells were treated with EdU for 4 hours. After incubation, media was removed and 1 mL of 4% paraformaldehyde in PBS was added to each well containing the coverslips for 15 minutes at room temperature. Cells were washed in each well twice with 1 mL of 3% BSA in PBS. 1 mL of 0.5% Triton® X-100 was added to each well, for 20 minutes at room temperature. Cells were washed twice with 1 mL of 3% BSA in PBS. 0.5 mL of Click-iT® reaction cocktail was added to each well containing a coverslip for 30 minutes at room temperature in dark. Cells were washed with 1 mL of 3% BSA in PBS. DNA stain 1X Hoechst 33342 solution (5 µg/mL) 1mL was added per well for 30 minutes at room temperature, protected from light. Remove the Hoechst 33342 solution. Cells were washed twice with 1 mL of PBS. A drop of Hydromount (Cat#NAT1324, National Diagnostics, Atlanta, GA, USA) was added to each glass slide (Cat# 12-550-15, Fisher Scientific, Waltham, MA). Coverslips were gently removed from 6 well plates using forceps and placed on the glass slides.

Images were acquired using Nikon Eclipse Ti inverted microscope using 20X objective and DAPI, GFP, fluorescent channels. Three images per replicate were taken for EdU and Hoechst

stained cells. Exposure settings were optimized for all channels in the NIS elements software with DAPI exposure 100ms, GFP 100ms.

Image Analysis

Images were analyzed using ImageJ 1.53t. DAPI Images were converted to 8 bit, followed by adjusting the threshold. EdU images were also converted to 8 bit and threshold adjusted. DAPI colocalization images were made using AND function in Image calculator. Cells were counted in DAPI and DAPI+EdU+ images using Analyze particles function. Cell counts were analyzed and bar graphs were created using GraphPad Prism 9.5.0.730.

Ki67 assay

Coverslips (Cat# 801011, Wuxi NEST Biotechnology, Jiangsu, China) were sterilized in 70% ethanol and placed in 6 well plates. Plates with coverslips were coated with 2 ml Matrigel for 1 hour at 37 C. Matrigel was aspirated and 200,000 cells were seeded in 2 ml appropriate media for the cells and left overnight in the CO2 incubator. Cells were treated with cortisol or DMSO for 24 hours in triplicates. Media was aspirated using glass pipette and cells were washed once with 1X PBS. Ki67 staining using Anti-Ki67 (Cat# ab15580, Abcam, Cambridge, UK) antibody was done according to the immunofluorescence protocol (described above). Data was analyzed as described in immunofluorescence (above).

Gene expression

RNA extraction for qPCR

NPCs and iPSCs were grown in 6 well plates. Cells were disrupted using 350µL Buffer RLT and cell scraper was used to detach cells. Lysates were collected in QIAshredder spin column placed in a 2 ml collection tube, and centrifuged for 2 minutes in full speed in eppendorf microcentrifuge. RNA was extracted from the lysates with RNeasy mini kit (Cat# 74104, Qiagen, Hilden, Germany)

RNA extraction for RNA sequencing

NPCs were grown in 6 well plates. Cells were disrupted using 700 µL QIAzol Lysis Reagent and cell scraper was used to detach cells. The collection of lysates was done using a QIAshredder spin column inside a collection tube of 2 ml capacity. The centrifugation process, which involved the use of an Eppendorf microcentrifuge, was carried out at maximum speed for a duration of 2 minutes. RNA was extracted using miRNeasy mini kit (Cat# 217004, Qiagen, Hilden, Germany) following kit instructions.

RNA quantification

RNA samples for quantification were prepared using RNA High sensitivity kit (Cat# Q32855, Thermo Fisher, Waltham, MA, USA) . To create the Qubit™ working solution, the Qubit™ RNA HS reagent was mixed with Qubit™ RNA HS buffer at a ratio of 1:200, resulting in a diluted solution. 2µL RNA sample was added to 198µL Qubit working solution. The samples were quantified using Qubit 4 Fluorometer. RNA samples were stored at -80 C.

RNA quality

Samples for Quality Assessment were prepared using RNA 6000 Nano kit. The chip priming station was prepared according to manufacturer's instructions. Electrodes were decontaminated, gel and gel-dye mix were prepared following kit instructions. The gel-dye mix was loaded on the chip with the help of chip priming station. 5µL RNA 6000 Nano Marker was added the wells as shown in the kit manual. 1µL Ladder or RNA samples were loaded on the chip. The chip was inserted into Agilent 2100 Bioanalyzer. Data was acquired using Agilent 2100 expert software. Electrodes were cleaned after chip run. RNA samples had RIN >9. RNA peaks were compared to the graphs (Figure 2.4).

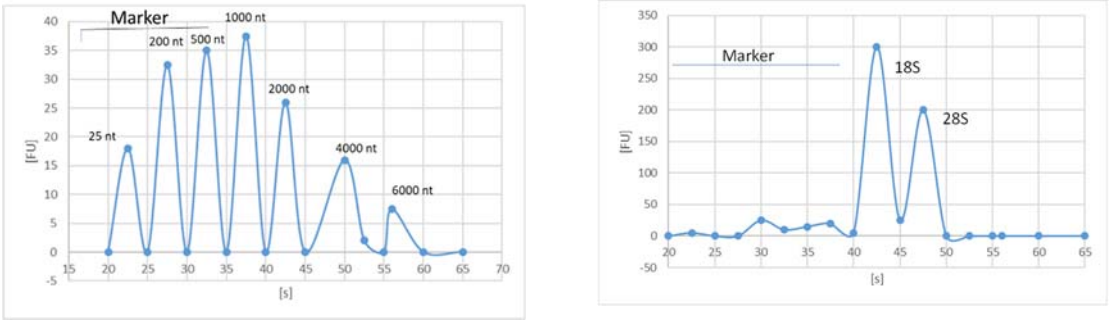

Figure 2.4: RNA 6000 Nano Ladder (Left) and RNA peaks of a successful sample run (right) (modified from https://www.agilent.com/cs/library/usermanuals/Public/G2938-90034_RNA6000Nano_KG.pdf)

cDNA synthesis

cDNA was synthesized using Reverse Transcription system (Cat# A3500, Promega, Madison, WI, USA) in MJ Research PTC-100 Thermal Cycler. 1µg Total RNA was incubated at 70 C for 10 minutes and centrifuged briefly in a microcentrifuge and placed in ice. A 20µl reaction was prepared by adding the following reagents: 25mM MgCl2, 4µl Reverse Transcription 10X Buffer, 2µl dNTP Mixture, 10mM 2µl Recombinant RNasin® Ribonuclease Inhibitor, 0.5µl AMV Reverse Transcriptase, Random Primers 0.5µg and total RNA 1µg. Nuclease-Free Water was added to make a final volume of 20µl. The reaction mix was incubated at room temperature for 10 minutes. In the thermal cycler, reaction mix was incubated at 42°C for 15 minutes. The sample was heated at 95°C for 5 minutes, then kept at 0–5°C for 5 minutes. cDNA samples were stored in -20 C.

Primer Design

The desired genome sequences were selected using UCSC genome browser (https://genome.ucsc.edu/cgi-bin/hgTracks). Exons shared between most of the isoforms were preferred sequences for primer design. mRNA transcript sequence of the selected isoform and exon positions were extracted from NCBI (https://www.ncbi.nlm.nih.gov/nuccore/). Primer sequences were generated using primer blast (includes exon-exon junction) https://www.ncbi.nlm.nih.gov/tools/primer-blast/. Several parameters such as Primer melting temperature ~60 C, GC content 40-60%, GC clamp, primer length 18-30 nt were used to select a

suitable primer pair. Amplicon sequence was derived from UCSC in silico PCR (https://genome.ucsc.edu/cgi-bin/hgPcr) and used to predict Melt curve of PCR product using Umelt (https://www.dna-utah.org/umelt/quartz/um.php.) Primer pair with single melt curve peak was selected. The list of primers used are included in Appendix.

qPCR

PCR reaction mix was prepared for each primer pair in a 1.5 ml Eppendorf tube with the following components (per well volume): SYBR Green Supermix (Cat# 1725271, Bio Rad, Hercules, CA, USA) 5µL, Forward primer 0.25µL, Reverse primer 0.25 µL , Water 3.5 µL. Final PCR reaction mix of 10µL total volume was prepared in 384 well plates (Cat# HSP3805, Bio Rad, Hercules, CA, USA) with 9µl PCR reaction mix (above) and 1µL cDNA or nuclease-free water (No Template control, NTC for each primer pair). The following steps were programmed in the CFX384 Touch Real-Time PCR System: Hot start 30 sec at 95 °C → 40 cycles(Denaturation at 95 °C → Annealing at 55 °C → Extension 72 °C) → Melting between 65-95 °C 0.5 °C increments 2-5 second/step. Data was acquired using CFX384 Touch Real-Time PCR System. PCR efficiencies were calculated using LinRegPCR, with efficiencies ranging from ~1.8 to 1.985. Relative normalized expression was determined using BioRad CFX Maestro 1.1 software with GAPDH and C1orf43 as reference for calculations.

RNA sequencing

Sequencing Library was prepared using Illumina® Stranded Total RNA Prep, Ligation with Ribo-Zero Plus (Cat# 20040525, Illumina, San Diego, CA, USA). 500ng RNA was used as input to the kit. Library quality was assessed using Agilent 2100 Bioanalyzer. The libraries were sequenced on the Illumina NextSeq 2000 instrument, with a paired end 2x100bp run. A total of 800M reads were generated ~80M total reads per sample.

RNA sequencing analysis

Quality Control , Trimming, Alignment and Quantification was done in Linux environment. Sequencing quality check was determined using FastQC. FastQC reports for all files were compiled using MultiQC. Read were trimmed using Trimmomatic with the following parameters – Leading – 3, Trailing – 3, Sliding window 4:15, Minlen – 36. FastQC Quality check after trimming was compiled using MultiQC. Reads were aligned with Gencode GRCh38 release r38

Human reference genome using STAR aligner. featureCounts package in subread program was used to count and annotate the reads that match with reference annotation . The filtering of genes was done by ensuring that they had a count per million (cpm) value of at least 1 in at least 4 samples. Following this, the data was normalized using the edgeR program to account for variations in library size. Batch effects were removed by ComBat in SVA R package. Differential genes were determined using Limma. Pathways were analyzed using KEGG in https://david.ncifcrf.gov/.

Protein Expression

Protein extraction

NPCs were seeded at 200,000 cells in 6 well plates using the NPC culture protocol (described above). Protease inhibitor - One complete Mini EDTA-free tablet (Cat# 11836170001, Millipore Sigma, Darmstadt, Germany) was dissolved in 1.5 ml mPER buffer (Cat# 78503, Thermo Fisher, Waltham, MA, USA) to make 7X stock solution. This solution was diluted to 1X in 1mL mPER buffer. Media was removed from the plate and 200µL mPER was added, and cell scraper was used to detach cells. The collection of lysate was done and then moved to a small tube for centrifugation. To remove the cell debris, the samples were spun at a speed of approximately 14,000 x g for a duration of 5 minutes. Supernatant was transferred to a new Eppendorf tube for quantification. Protein samples were stored in -80C.

Protein quantification

Protein Broad Range Assay kit (Cat# A50668, Thermo Fisher, Waltham, MA, USA) was used to prepare samples. 20µL protein sample was added to assay tube, followed by 150µL protein BR assay buffer and 30µL protein BR assay reagent. Samples were kept at room temperature for 10 minutes followed by protein measurement using Qubit 4 Fluorometer (Cat# Q33238, Thermo Fisher, Waltham, MA, USA).

Western Blot

mPER was used as the diluent to make sample concentrations equal. Samples were diluted 1:3 in 4x Laemmli Sample Buffer (Cat#1610747, Bio Rad, Hercules, CA, USA). Protein samples were heated for 5 min at 95 C using heat block. Gel 4–20% Mini-PROTEAN® TGX Stain-Free™

Protein Gels, 12 well, 20 µl capacity (Cat#4568095, Bio Rad, Hercules, CA, USA) was placed in Mini-PROTEAN® Tetra Electrode Assembly (Cat# 1658037, Bio Rad, Hercules, CA, USA) and fixed in the gel tank. Mini Cell Buffer Dam (Cat#1653130, Bio Rad, Hercules, CA, USA) was fixed on one side of the assembly if running one gel. Running buffer – 1X Tris/Glycine/SDS (Cat#1610732, Bio Rad, Hercules, CA, USA) was added in the space between the gels. Comb was removed before loading samples. 5µL Ladder - Precision Protein Dual Color (Cat#1610374S, Bio Rad, Hercules, CA, USA) was loaded on to one well of the gel. 20 µl samples were loaded in the preferred order. Running buffer (Cat#1610732, Bio Rad, Hercules, CA, USA) was added to the gel tank till the level marked on the tank. Power Supply was programmed and connected to the electrodes; run was started at 100V for ~2 hours. Transfer cassette was prepared and transfer assembly was prepared using transfer kit (Cat#1704270, Bio Rad, Hercules, CA, USA) as shown below (Figure 2.5). 1X Transfer buffer (Cat#1704270, Bio Rad, Hercules, CA, USA) was used to prepare wet stacks. Gel was transferred to the membrane. Proteins were transferred using Trans-Blot Turbo Transfer System (Cat#1704150, Bio Rad, Hercules, CA, USA) for 20 minutes on mixed molecular weight program. The membrane was transferred to a box filled with EveryBlot Blocking Buffer (Cat#12010020, Bio Rad, Hercules, CA, USA) for 1 hour on a plate shaker. Primary antibodies were added at the desired concentrations and kept overnight in the cold room on a shaker. Wash buffer was prepared by adding 1mL Tween (Cat# P1379, Sigma Aldrich, Darmstadt, Germany) to 1X Tris Buffered Saline (TBS) (Cat#1706435, Bio Rad, Hercules, CA, USA). Next day, membranes were washed 3 times with 10 mL wash buffer for 10 minutes each time at room temperature on plate shaker. Secondary antibodies were diluted in blocking buffer and added to the membranes for 1 hour at room temperature on a shaker. Membranes were washed 3 times with 10 mL wash buffer for 10 minutes each time in room temperature on plate shaker. Imaging solution - Clarity™ Western ECL Substrate (Cat#1705060, Bio Rad, Hercules, CA, USA) was prepared and 1 ml was added to the membrane and image acquisition was started. Membrane was visualized using chemiluminescence in Bio-Rad ChemiDoc system. Images were analyzed using Image Lab 6.1.

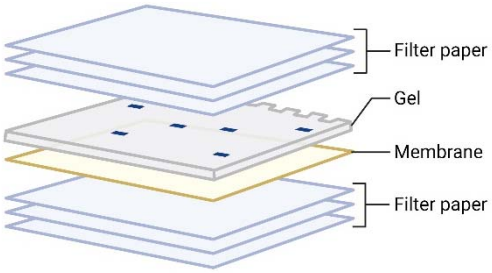

Figure 2.5: Membrane assembly for transfer of proteins to blot

Statistical Analysis

Statistical analysis was done using t tests in Graph Pad Prism 9.5.0.730. p values < 0.05 was considered as significant. There is no specific sample size requirement for t test. ANOVA or the non-parametric equivalent test Kruskal-Wallis could not be used for this study due to the low power which will reduce the possibility to detect differences between sample means.

RESULTS

3.1 Human iPSCs were differentiated to NPCs using STEMCELL Technologies SMADi protocol.

Human iPSCs expressed SSEA4 on their surface (undifferentiation marker) based on immunofluorescence (Figure 3.1). iPSCs were differentiated to NPCs using the protocol from STEMCELL Technologies (described in Methods). iPSCs were plated as single cells and began to show morphological changes around Day 11 when cells began to look more like NPCs and began proliferating (Figure 3.2). At Day 23, we obtained NPCs and characterized the cells further using qPCR and immunofluorescence for NPC markers. Marker genes used to characterize iPSCs, NPCs and Neurons are listed in Table 3.1.

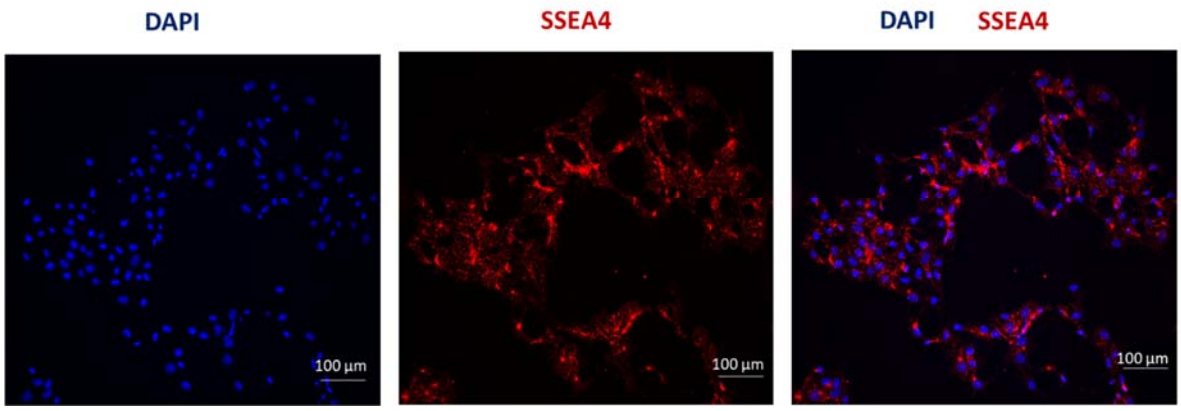

Figure 3.1: SSEA4 immunostaining in iPSCs

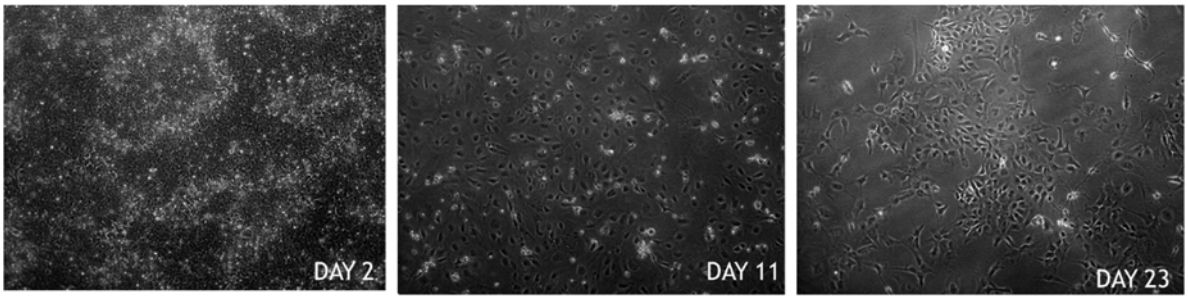

Figure 3.2: Phase contrast images - iPSC to NPC differentiation

Table 3.1: Marker genes to characterize iPSC, NPC and Neurons

	Gene
iPSC	SSEA4, SOX2
NPC	SOX2
	Nestin
	PAX6
	SOX1
Neuron	MAP2
	NeuN

3.2 NPC differentiation was confirmed by marker gene and protein expression.

iPSCs and NPCs were stained for SOX2, Nestin, PAX6, SOX1 (Figure 3.3, 3.4,3.5). iPSCs and NPCs expressed SOX2 and Nestin based on immunofluorescence. SOX2 is a transcription factor and is localized in the nucleus in iPSCs and NPCs (Figure 3.3). Nestin is an intermediate filament protein and is present in cytoskeleton in both iPSCs and NPCs (Figure 3.3). PAX6, a transcription factor, is expressed in iPSCs and NPCs, however, PAX6 is nuclear in NPCs but it is both nuclear and cytoplasmic in iPSCs (Figure 3.4). SOX1, also a transcription factor, is expressed in both iPSCs and NPCs. SOX1 is nuclear in iPSCs and NPCs (Figure 3.5). Nearly

>90% NPCs expressed SOX2, PAX6 and SOX1 (Figure 3.7). NPCs did not express SSEA4, undifferentiation marker (Figure 3.6). SSEA4 expression in iPSCs was confirmed by immunofluorescence (Figure 3.1).

SOX2, Nestin, PAX6 and SOX1 mRNA expression was quantified in iPSCs and NPCs (Figure 3.8). iPSCs and NPCs express SOX2 based on qPCR analysis. There was no difference between the relative SOX2 expression in iPSCs and NPCs. However, relative NES, PAX6 and SOX1 mRNA expression levels showed a visible increase in NPCs compared to iPSCs based on the graph, although it is not significant ($p = 0.092652$ (NES) , 0.129143 (PAX6) , 0.063387 (SOX1)) (Figure 3.8). SOX2, NES, PAX6 and SOX1 expression in iPSCs and NPCs were also confirmed by Cq values < 30 (Appendix). The summary of marker mRNA and protein expression in iPSCs and NPCs is presented in the table below (Table 3.2). Results that were found to be inconsistent with reported literature are highlighted in the table and will be discussed in the next section.

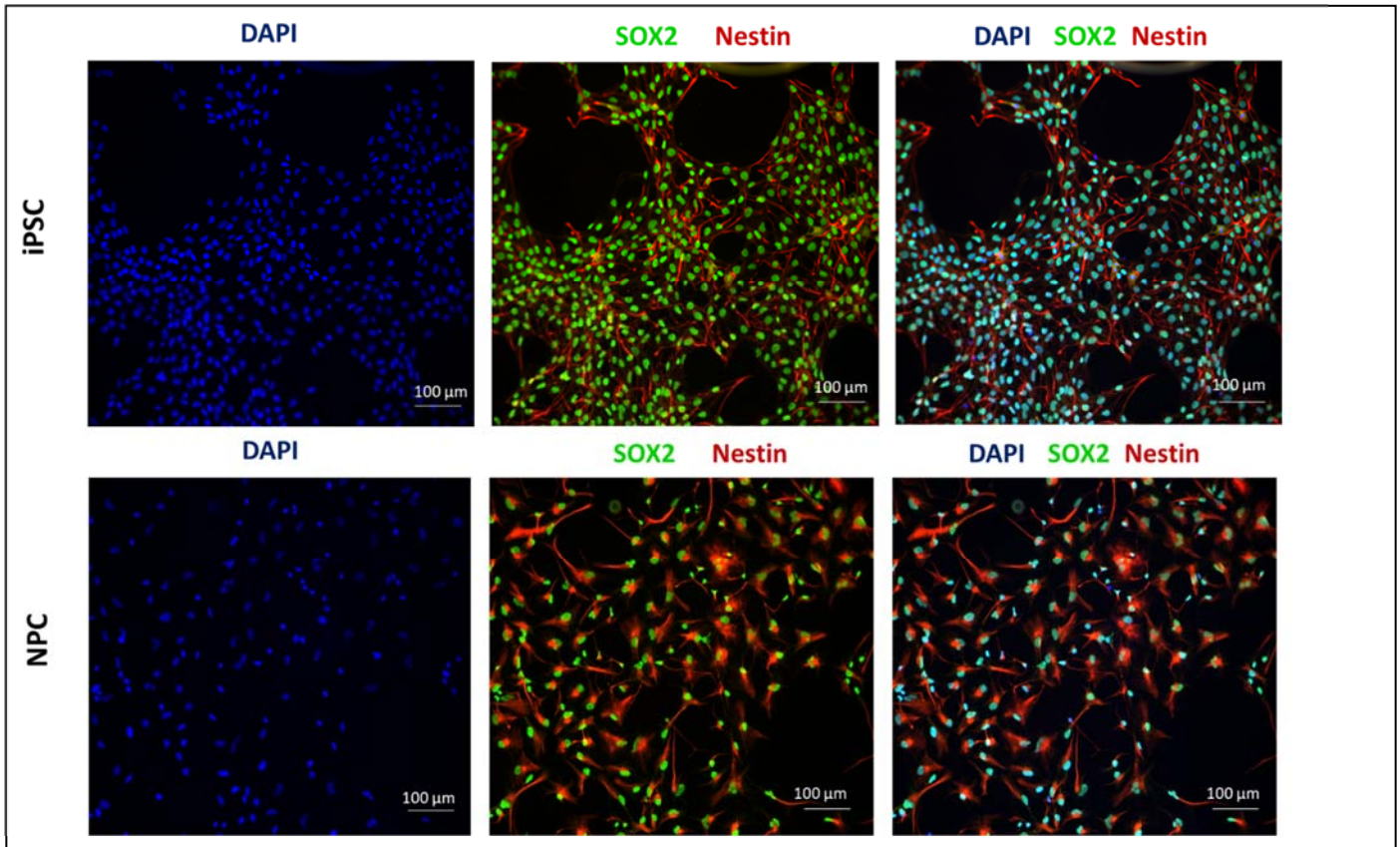

Figure 3.3: SOX2 and Nestin immunostaining in iPSCs and NPCs

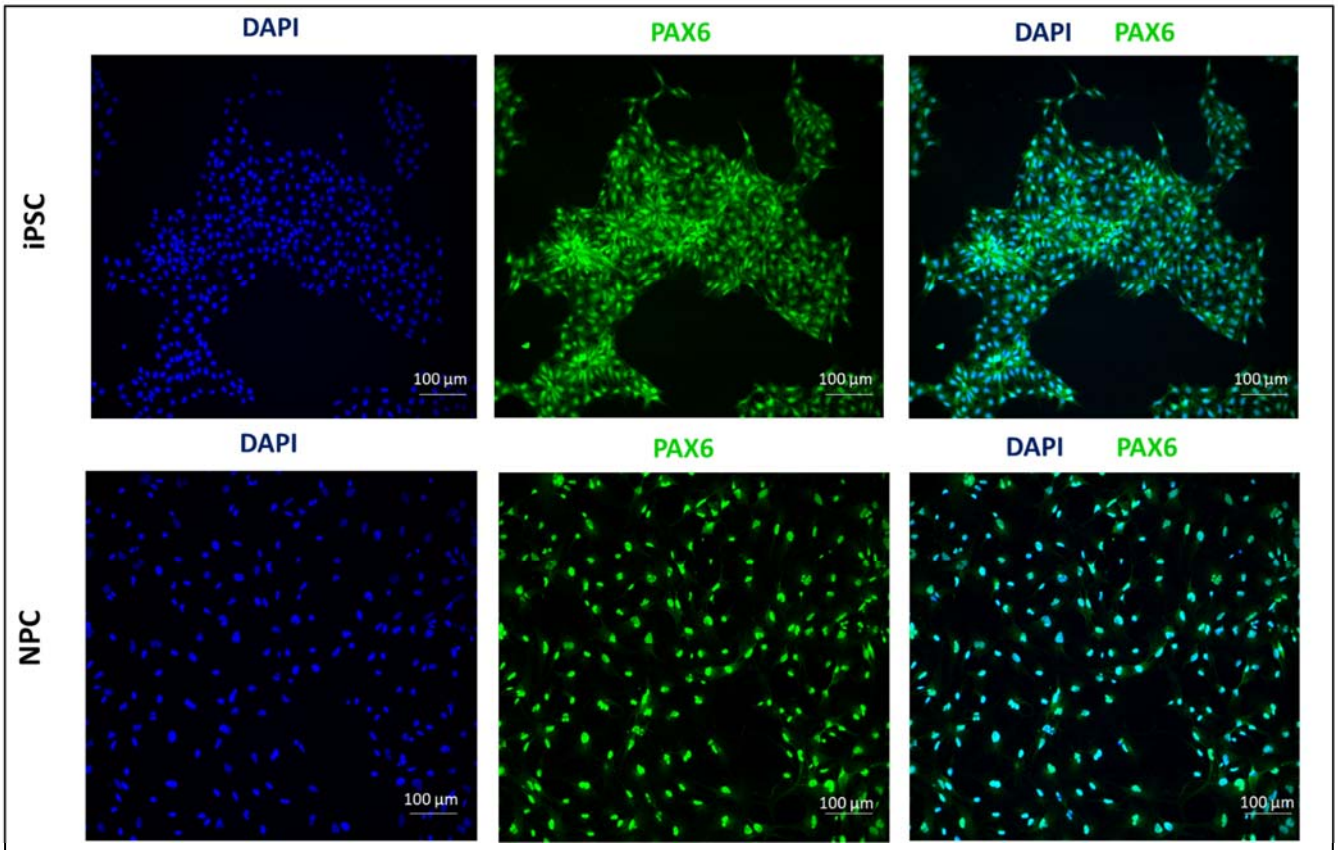

Figure 3.4: PAX6 immunostaining in iPSCs and NPCs

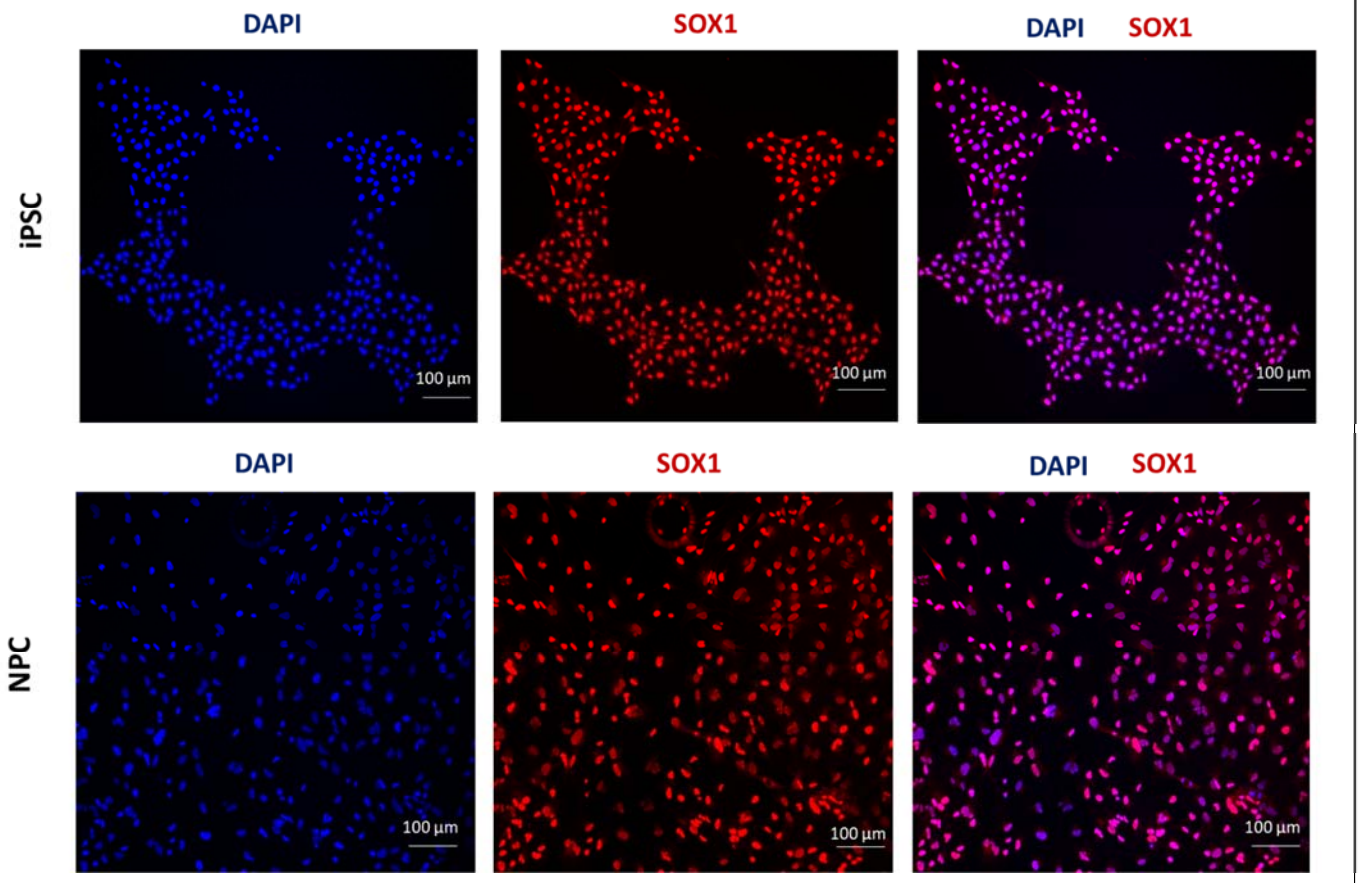

Figure 3.5: SOX1 immunostaining in iPSCs and NPCs

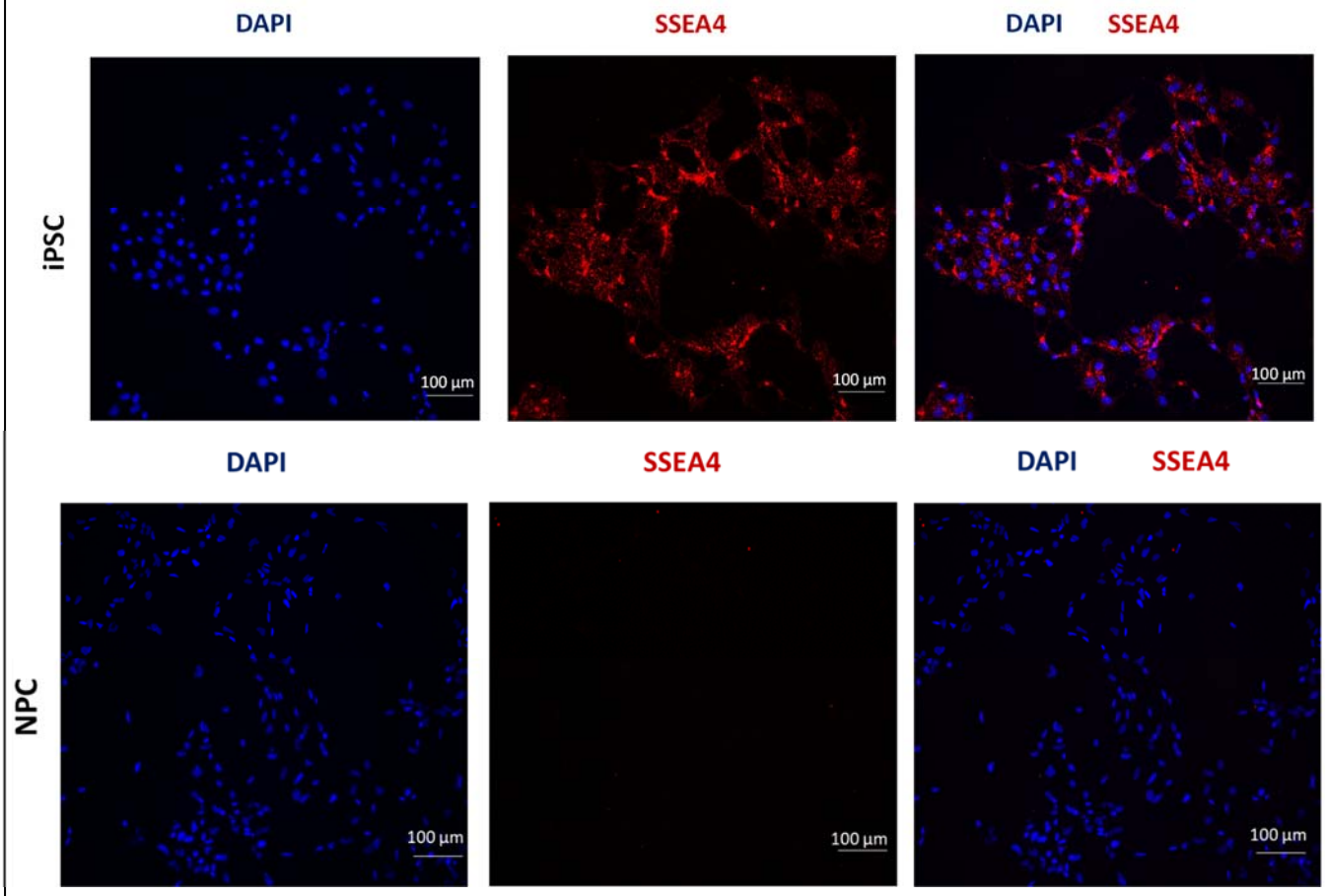

Figure 3.6: SSEA-4 immunostaining in iPSCs and NPCs

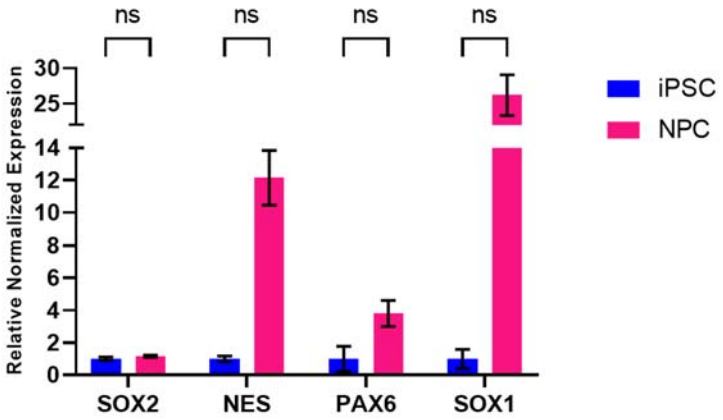

Figure 3.7: Percentage of NPCs expressing SOX2, PAX6 and SOX1 based on immunofluorescence data (above). Data shows Mean+ SE, n = 2 per group.

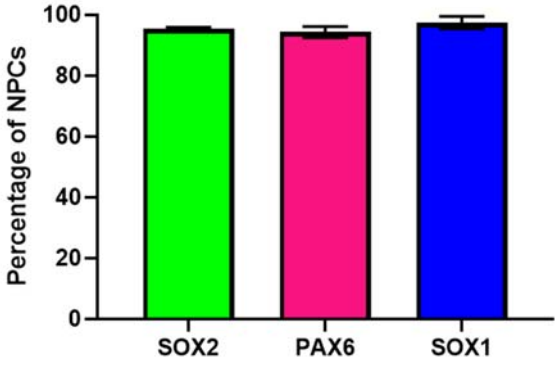

Figure 3.8: Relative mRNA expression of SOX2, NES, PAX6 and SOX1 based on qPCR (above). Data shows Mean+SE, n = 3 per group.

Table 3.2: Summary of iPSC and NPC marker gene and protein expression

Marker Expression	**iPSC (Gene) qPCR**	**NPC (Gene) qPCR**	**iPSC (Protein/Localization) Immunofluorescence**	**NPC (Protein/Localization) Immunofluorescence**
SSEA4	not tested	not tested	+/Cell Surface	-
SOX2	+	+	+/Nuclear	+/Nuclear
NES	+	++	+/Cytoplasm	+/Cytoplasm
PAX6	+	++	+/Cytoplasm/Nuclear	+/Nuclear
SOX1	+	++++	+/Nuclear	+/Nuclear

Yellow highlighted the results inconsistent with previous publications.

3.3 Novel isoforms of Nestin could be present in NPCs but not in iPSCs.

During marker gene expression analysis (3.2), the original primer designed to amplify NES (NES 1) , did not amplify any region in NPCs. However, there was amplification in iPSCs (Cq values shown in Appendix Figure 1 and Amplification curve shown in Appendix Figure 2). Therefore, new set of primers NES 2 and NES 3 were designed (Appendix Table 1) to study whether there was any amplification in NPCs. NES 2 and NES 3 showed amplification in NPCs and iPSCs (Figure 3.9). The amplification regions for NES 1, NES 2 and NES 3 are explained in Figure 3.9. NES 1 amplified the region between exon 1 and exon 2, while NES 2 and NES 3 amplified the region between exon 3 and 4. NES 1, 2 and 3 primers were designed using the only known transcript sequence ENST00000368223.4. However, IGV visualization of RNA seq data from NPCs (Section 3.8) showed differences in transcripts after aligning RNA sequencing files. There were several NES transcripts with shorter exons than expected.

Recent unpublished findings from Pinto Lab found novel NES short isoforms in adult human brain iso-seq data (Appendix Figure 3). There were 3 short NES isoforms that completely lack exon 1 in addition to other short NES isoforms with partial exon expression in this data. Fetal brain single cell Iso-seq data (unpublished) for NES was obtained from Gandal Lab. Two novel NES isoforms were identified in this data.

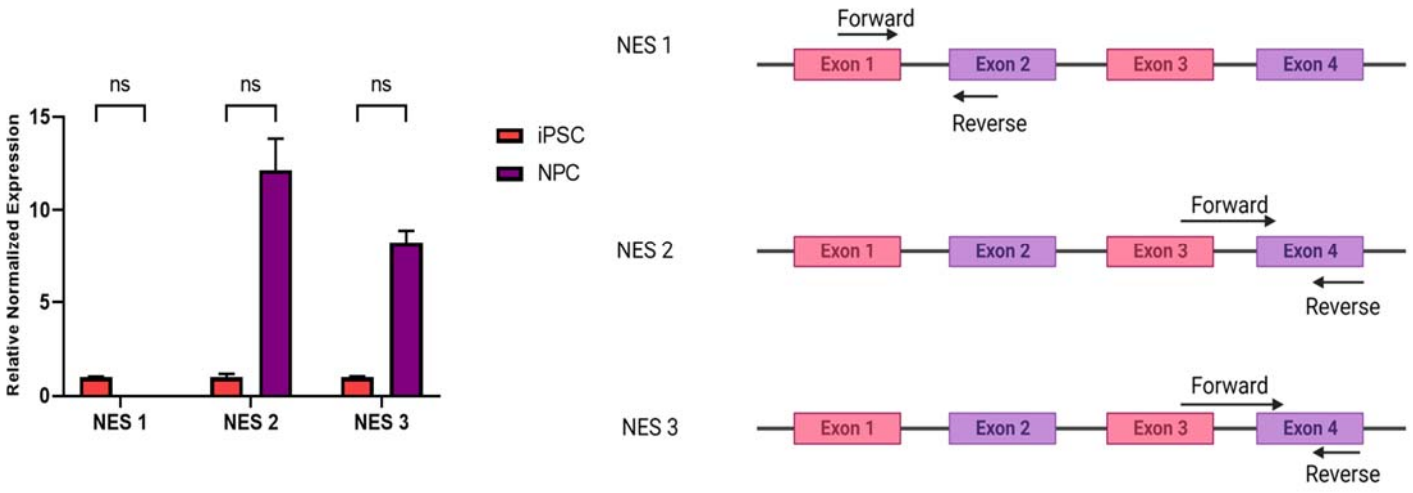

Figure 3.9: NES mRNA expression measured by qPCR ns: p>0.05 (left), NES Primer amplification regions (right). Data shows Mean±SE, n = 2 per group.

3.4 Glucocorticoid treatment induced elevated GC response mRNA expression in human iPSC derived NPCs.

NPCs were treated with DMSO, 0.5µM, 1µM, 3µM cortisol or 0.1µM Dexamethasone for 24 hours, followed by RNA extraction, cDNA isolation and qPCR measurements of FKBP5, ZBTB16, TSC22D3 and BDNF according to the experimental design in Figure 3.10. Expression was normalized to housekeeping genes GAPDH and C1orf43. FKBP5 mRNA expression did not increase significantly after cortisol treatment (Figure 3.11). There was significant increase in ZBTB16 mRNA expression after 0.5µM cortisol (p=0.0406) and 3µM cortisol (p=0.018930) treatment in NPC line 2 compared to DMSO treatment. 1µM cortisol, 0.1µM DEX treatment in NPC line 2 and cortisol treatment in NPC line 1 did not elevate ZBTB16 mRNA expression. There was significant increase in TSC22D3 mRNA expression after 0.5µM cortisol (p=0.0494) and 3µM cortisol (p=0.023873) treatment in NPC line 1 and 2 respectively compared to DMSO treatment. 1µM cortisol, 0.1µM DEX treatment in did not elevate TSC22D3 mRNA expression. BDNF mRNA expression decreased significantly after 0.1µM Dexamethasone (p=0.0352) and increased after 1µM cortisol (p=0.0232) treatment in NPC line 1 compared to DMSO treatment. However, cortisol treatment in NPC line 2 did not increase BDNF mRNA expression.

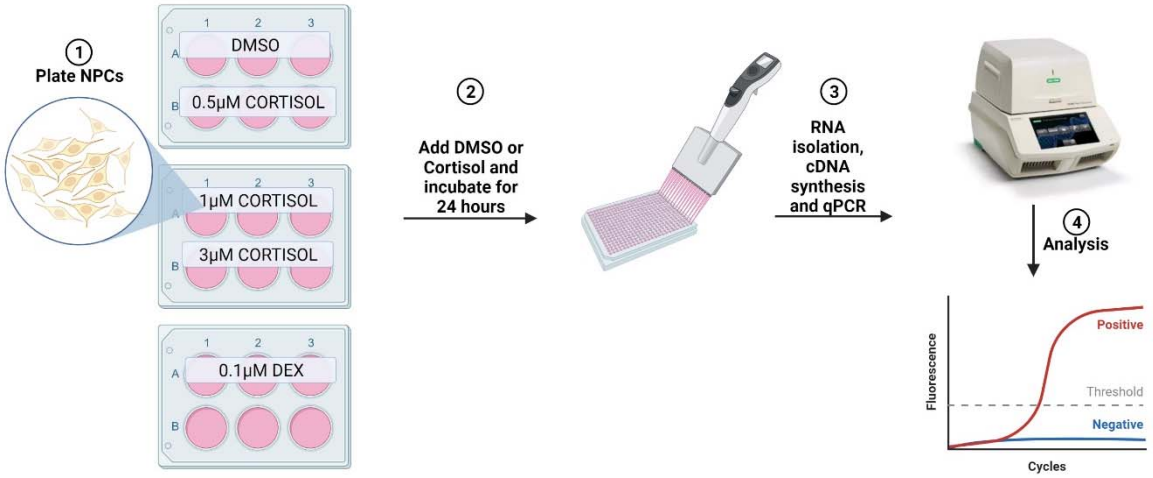

Figure 3.10: Experimental Design of cortisol treatment and qPCR measurement of GC response genes – FKBP5, ZBTB16, TSC22D3 and BDNF.

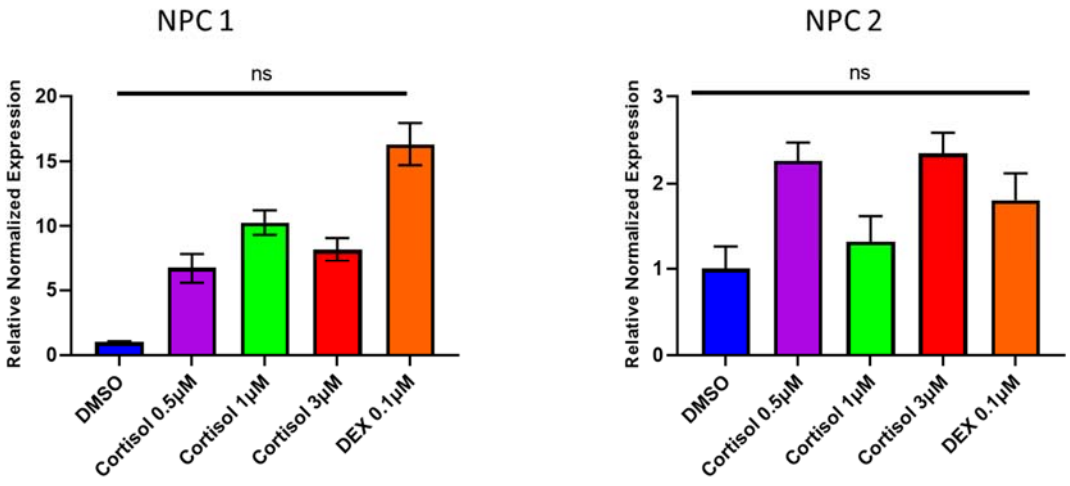

Figure 3.11: FKBP5 mRNA expression measured by qPCR ns: $p>0.05$. Data shows Mean± SE, n = 2 per group.

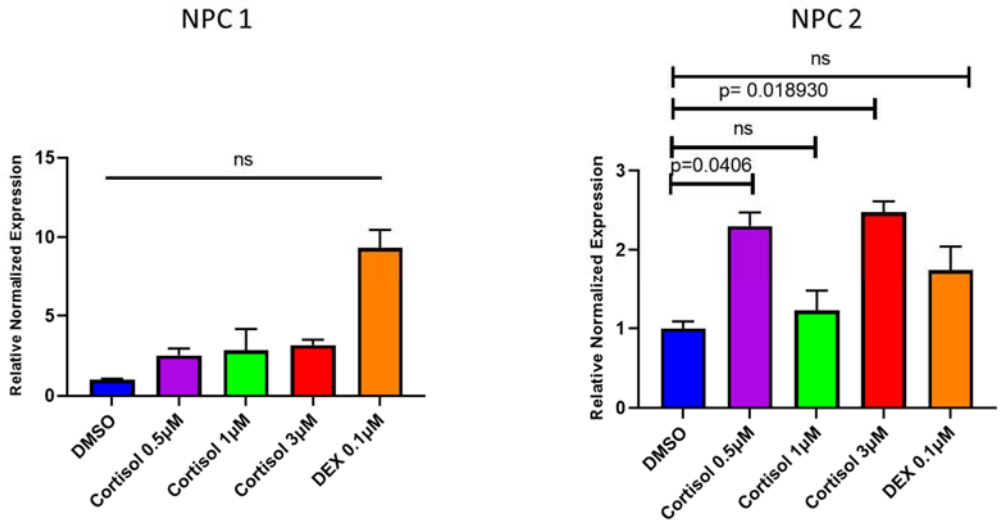

Figure 3.12: ZBTB16 mRNA expression measured by qPCR ns: p>0.05. Data shows Mean±SE, n = 2 per group.

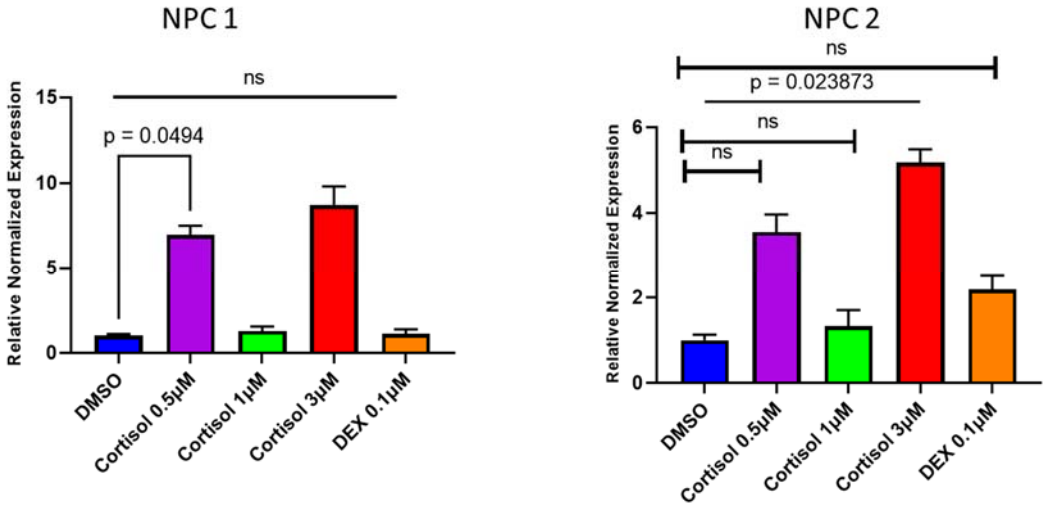

Figure 3.13: TSC22D3 mRNA expression measured by qPCR ns: p>0.05. Data shows Mean±SEM, n = 2 per group.

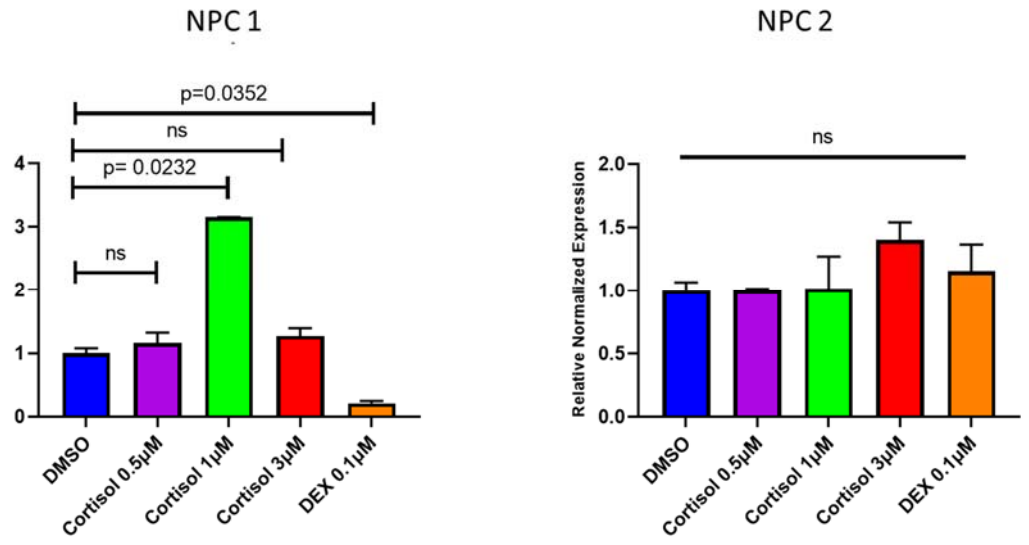

Figure 3.14: BDNF mRNA expression measured by qPCR ns: p>0.05. Data shows Mean±SEM, n = 2 per group.

3.5 Cortisol did not affect NPC viability.

NPC viability was measured using two methods – MTS assay and Live/Dead staining. NPCs were treated with DMSO or cortisol 3µM for 24 hours and MTS reagent was added followed by cell viability measurement (Methods, Figure 3.15). NPC viability was not affected by cortisol treatment (Figure 3.16).

Similarly, for live/dead staining, NPCs were treated with DMSO or cortisol 3µM for 24 hours followed by collecting cells and media for viability measurements (Figure 3.17). Live/Dead staining of cortisol treated NPCs did not show a significant change in viability (Figure 3.18).

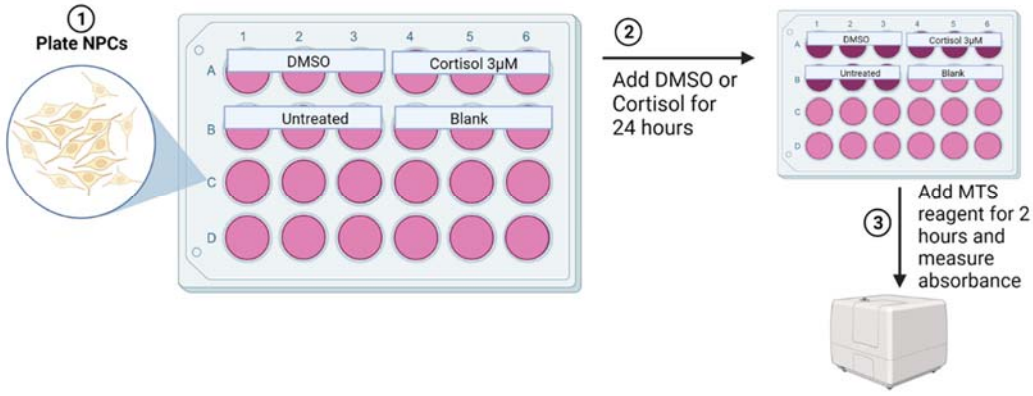

Figure 3.15: Experimental Design for MTS Assay to measure cell viability.

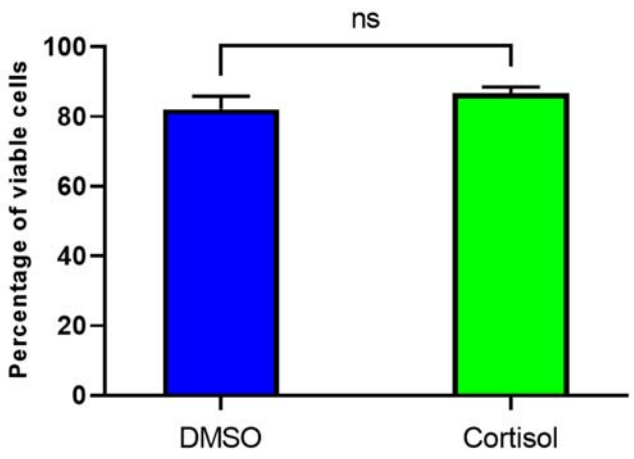

Figure 3.16: NPC viability after DMSO (left) or cortisol 3µM treatment for 24 hours. (right) , using MTS assay. Data shows Mean±SEM, n = 2 per group.

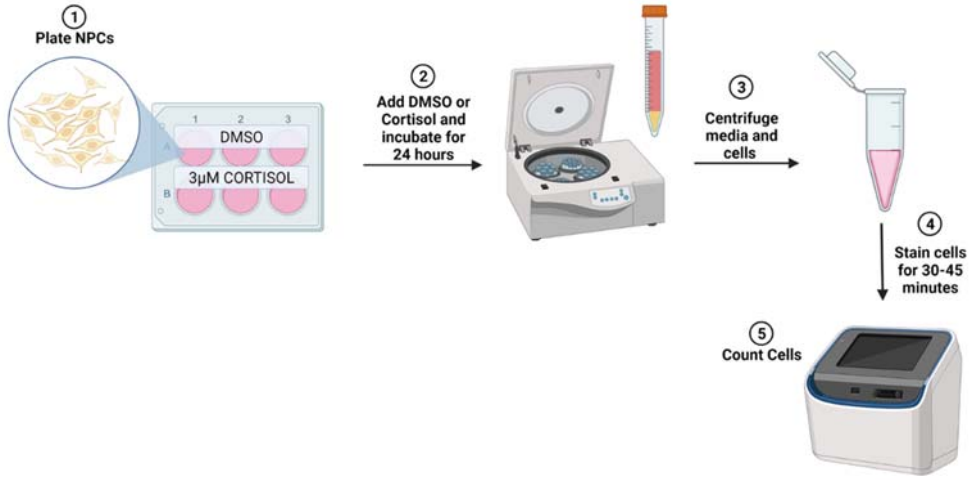

Figure 3.17: Experimental Design for Live/Dead Assay to measure cell viability.

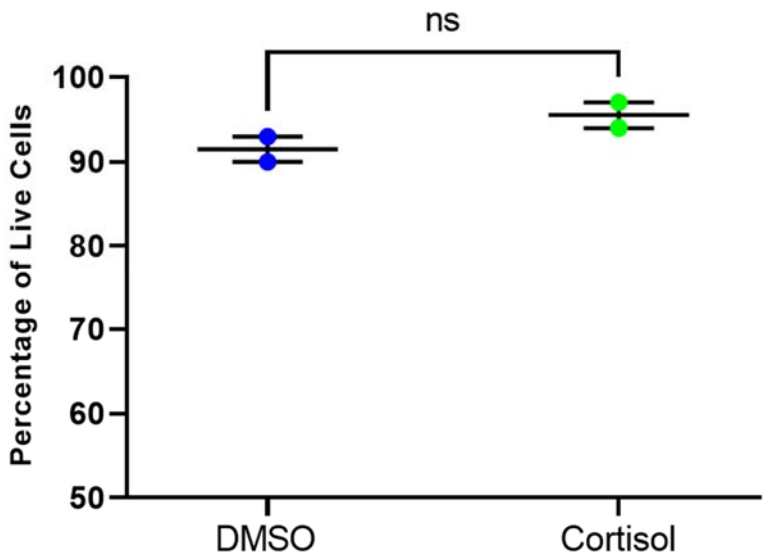

Figure 3.18: NPC viability after DMSO (left) or cortisol 3µM treatment for 24 hours. (right) , using Live Dead assay. Data shows Mean+ SEM, n = 2 per group.

3.6 Cortisol did not impact NPC proliferation.

NPC proliferation was measured using two methods – Ki67 expression and EdU staining. NPCs were treated with DMSO or cortisol 3µM for 24 hours and Ki67 expression was quantified (Figure 3.19). The percentages of Ki67 positive cells were quantified. DAPI was used to label nuclei. There was no visible change in Ki67 expression in cortisol treated NPCs compared to DMSO (Figure 3.20). Ki67 expression did not increase significantly after cortisol treatment compared DMSO treatment (Figure 3.21).

An alternative method to measure proliferation using EdU staining was established (Figure 3.22). EdU incubation period was optimized to 4 hours. DAPI was used to label nuclei. Immunofluorescence based imaging was used to detect EdU signal (Figure 3.23). Between 30% to 40% cells were EdU positive after 4 hour EdU incubation. Effect of cortisol treatment on NPC proliferation was not determined using this method.

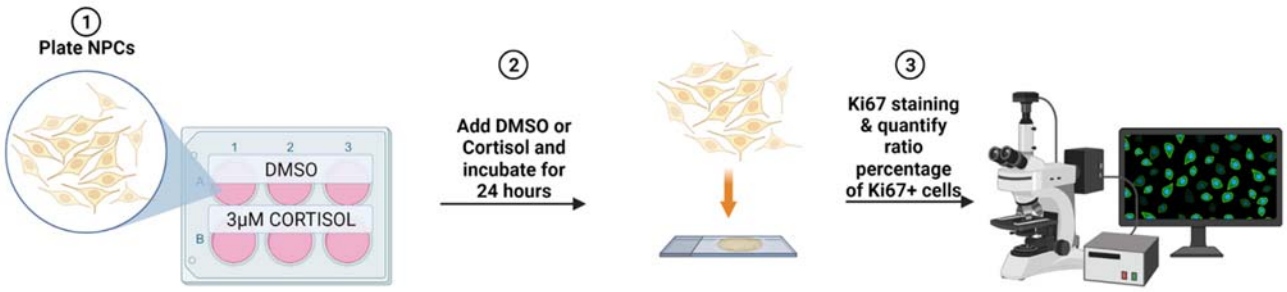

Figure 3.19: Experimental Design for Ki67 immunostaining to measure cell proliferation.

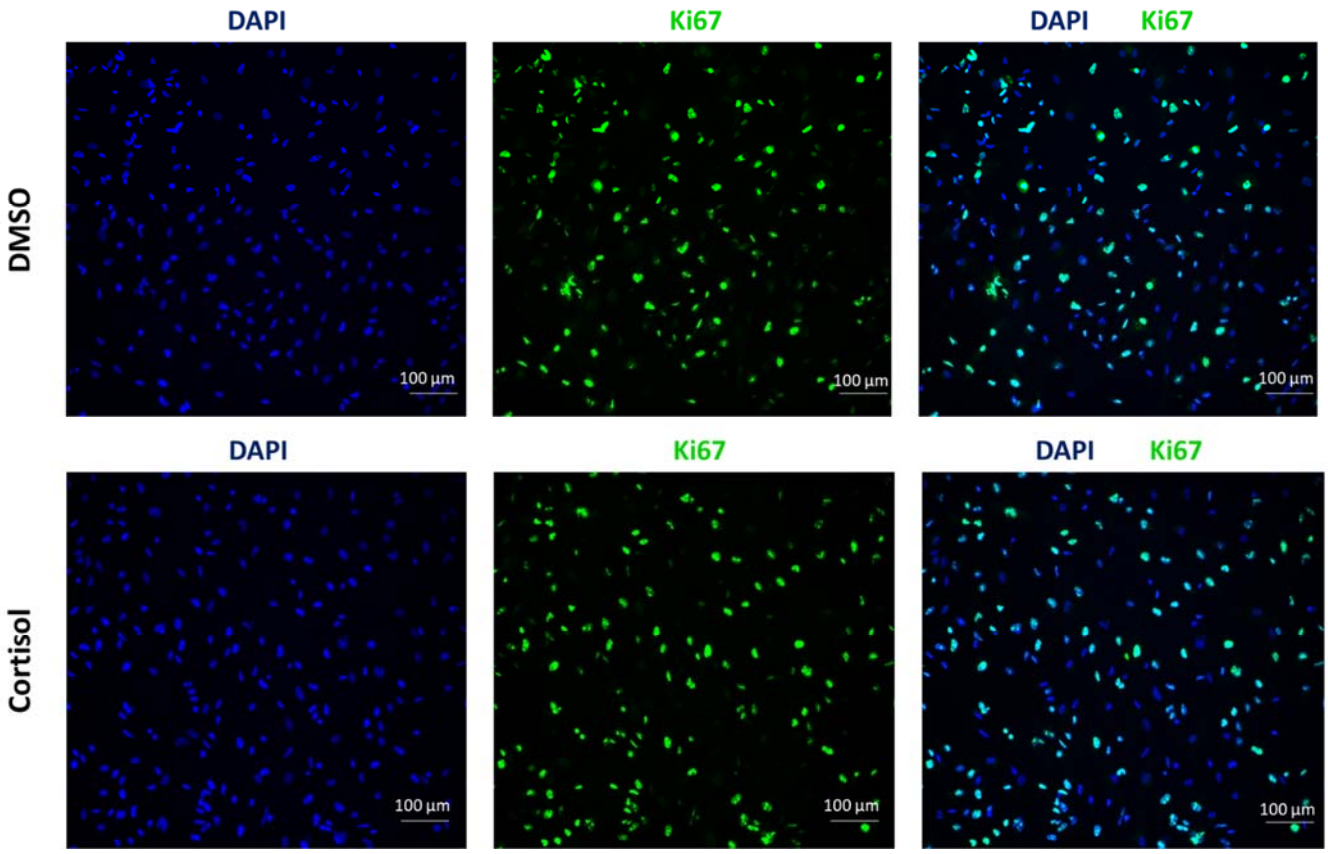

Figure 3.20: Ki67 expression after DMSO or cortisol 3µM treatment in NPCs for 24 hours.

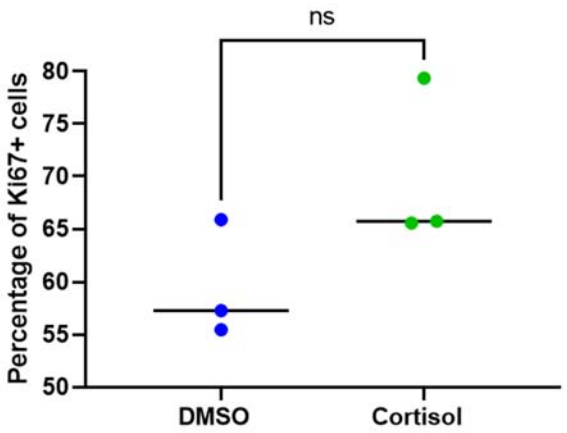

Figure 3.21: Ki67 quantification of NPCs after DMSO (left) or cortisol 3µM treatment for 24 hours. Data shows Mean, n = 2 per group.

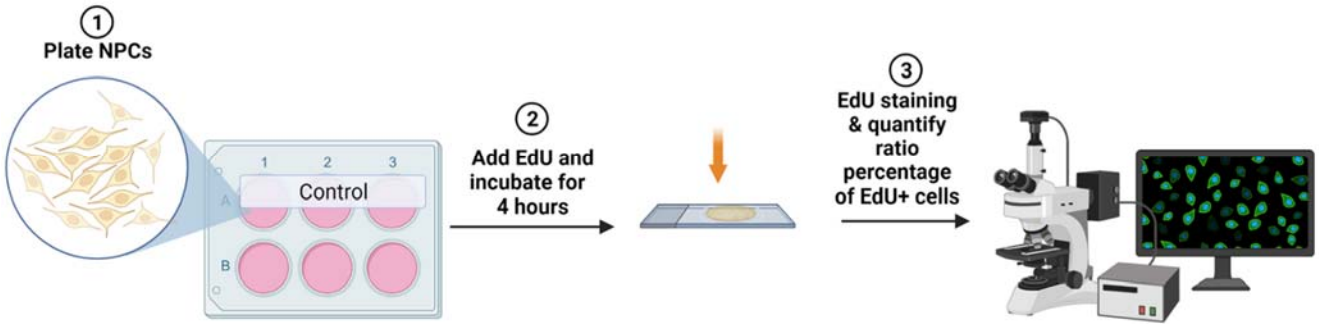

Figure 3.22: Experimental Design for EdU staining to measure cell proliferation.

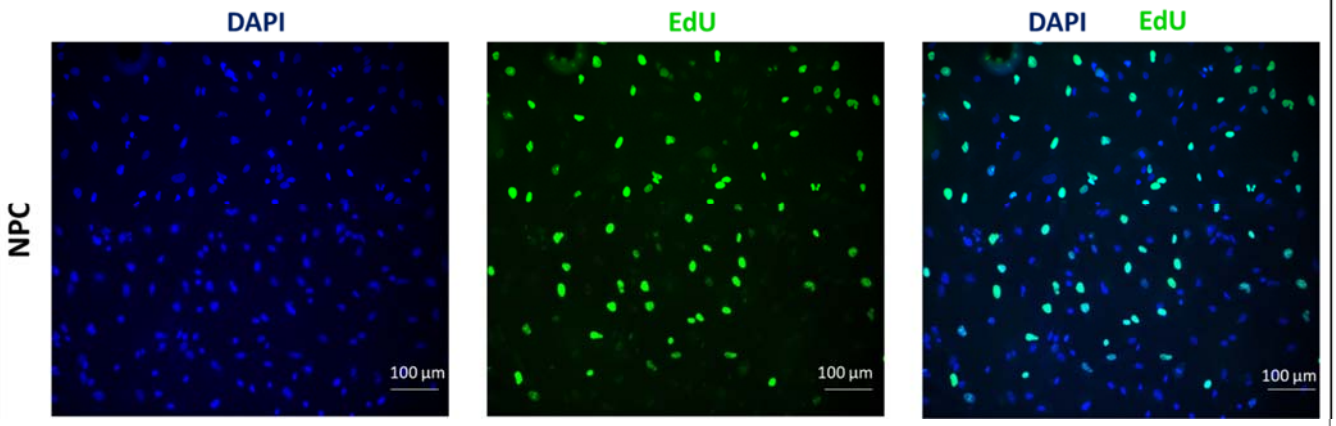

Figure 3.23: EdU staining after 4 hours EdU incubation in DMSO or Cortisol 3µM treated NPCs.

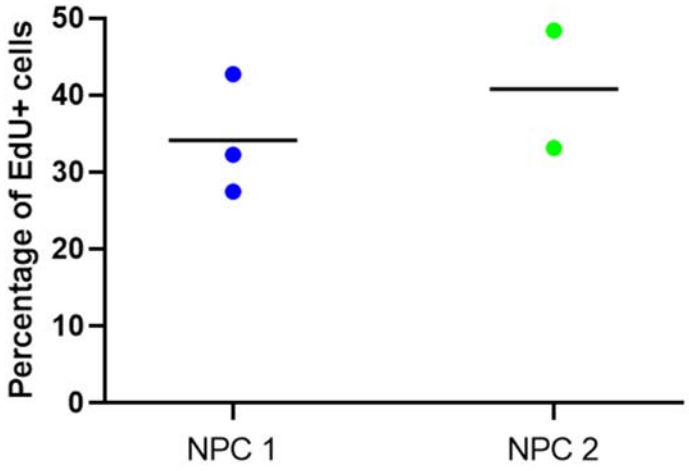

Figure 3.24: NPCs quantified based on EdU staining after DMSO (left) or cortisol 3μM (right) treatment for 24 hours. Data shows Mean, n = 2 per group.

3.7 Cortisol did not increase FKBP5 expression in NPCs.

NPCs were treated with either DMSO or cortisol 3μM for 24 hours followed by protein extraction (Figure 3.25). Western blot analysis showed equal GAPDH expression in NPCs. SH-SY5Y cells were used as control for GAPDH and FKBP5 protein measurement. GAPDH was used as a loading control. cortisol treatment did not increase FKBP5 protein expression in NPCs compared to DMSO treatment (Figure 3.26).

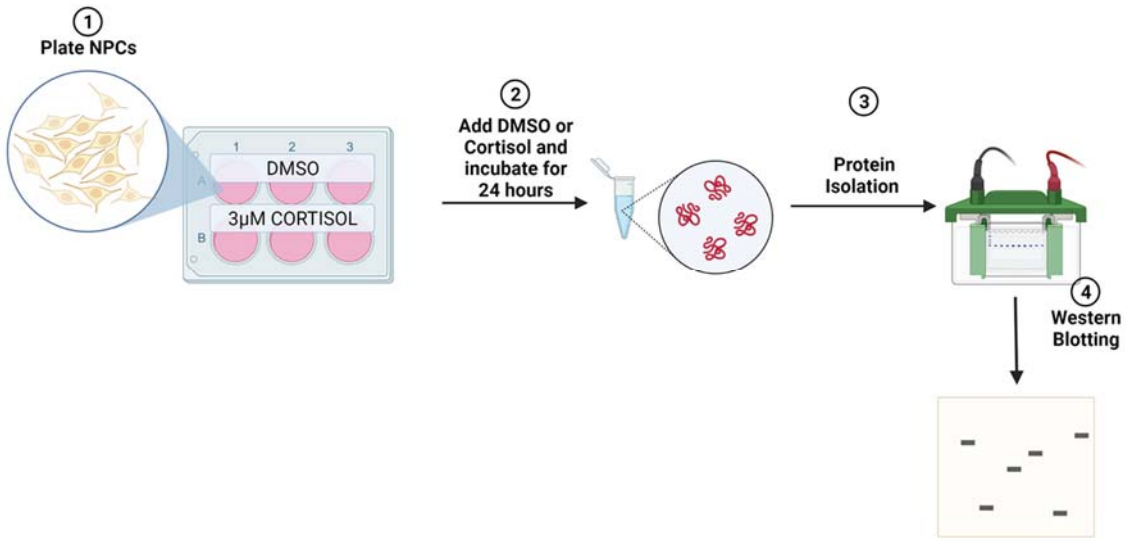

Figure 3.25: Experimental Design to measure protein expression using Western Blot.

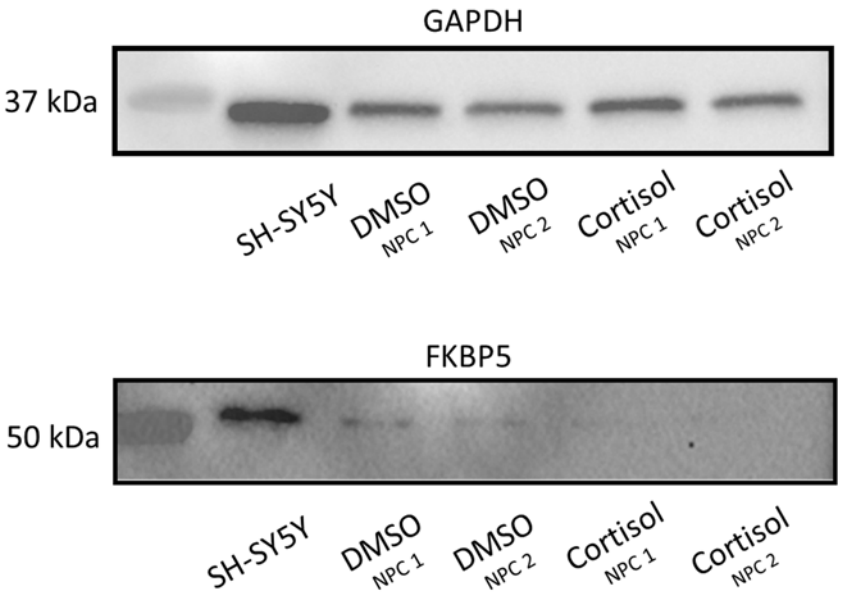

Figure 3.26: GAPDH and FKBP5 protein expression in NPCs after DMSO (left) or cortisol 3μM (right) treatment for 24 hours.

3.8 Cortisol induced changes in NPC transcriptome, pathways and differential expression of genes related to psychiatric traits.

NPCs from 2 biological replicates were treated with DMSO, 0.5µM, 1µM, 3µM cortisol or 0.1µM Dexamethasone for 24 hours, followed by RNA extraction, quality measurements, library preparation and sequencing (Described in methods and Figure 3.27). RNA quality was measured as RIN (RNA integrity number). All samples had RIN > 9 (Appendix Figure 6). Paired end sequencing files were received in Fastq format. Per base quality scores were determined using FastQC quality analysis. FastQC analyzed several metrics in the Fastq files, and data was compiled in MultiQC (Data not shown). The mean quality scores were >30 for all samples (Appendix Figure 7). After trimming the reads based on quality scores, reads were aligned to GRCh38 Human reference genome using STAR. Read quantification, normalization and filtering was done according to the protocol described in methods. A summary of the steps involved in RNA sequencing analysis is shown in Figure 3.28. After normalizing and filtering, batch effects were adjusted using Combat in SVA. However, post Combat, results did not account for the batch effects. PCA plot of the different samples showed a large variation between the four samples – DEX 0.1µM and cortisol 1µM treatment in NPC 1 and 2 (Figure 3.29). Furthermore, these four samples failed statistical model fitting to detect differential gene expression using Limma. Therefore, Four out of ten samples were removed from further differential gene expression analysis.

Differential genes were detected using quasi-likelihood F tests method in edgeR. 59 genes were differentially expressed in the comparisons between cortisol 0.5µM , 3µM and Control . 21 DEGs genes were shared between cortisol 0.5µM and 3µM treated NPCs (Figure 3.30 and Table 3.3). There were 5 unique DEGs after cortisol 0.5µM treatment and 33 unique DEGs identified in cortisol 3µM treated NPCs. ZBTB16 and TSC22D3 were differentially expressed in both cortisol 0.5µM and 3µM treated NPCs. ZBTB16 and TSC22D3 also had a fold change >2 after cortisol treatment compared to control. Previously (3.3), ZBTB16 and TSC22D3 mRNA expression were significantly increased after cortisol treatment which was determined using qPCR. DEGs were tested for pathway association using KEGG. KEGG analysis identified genes involved in Focal adhesion, cellular senescence and human papillomavirus pathways were shared between cortisol 0.5µM and 3µM treated NPCs (Table 3.4 and 3.5). All 59 genes were analyzed

for GWAS association using GWAS atlas (Table 3.6). 9 genes had significant ($p<10^{-8}$) associations with psychiatric traits. ZBTB16 was associated with anxious feelings, while PER1 was associated to chronotype and worry. PER1, POU2F2 and ZHX3 were associated with chronotype and morningness. FOSL1, TENM4, SORT1 and KLF9 were associated with educational attainment. These results will be discussed further in the next section.

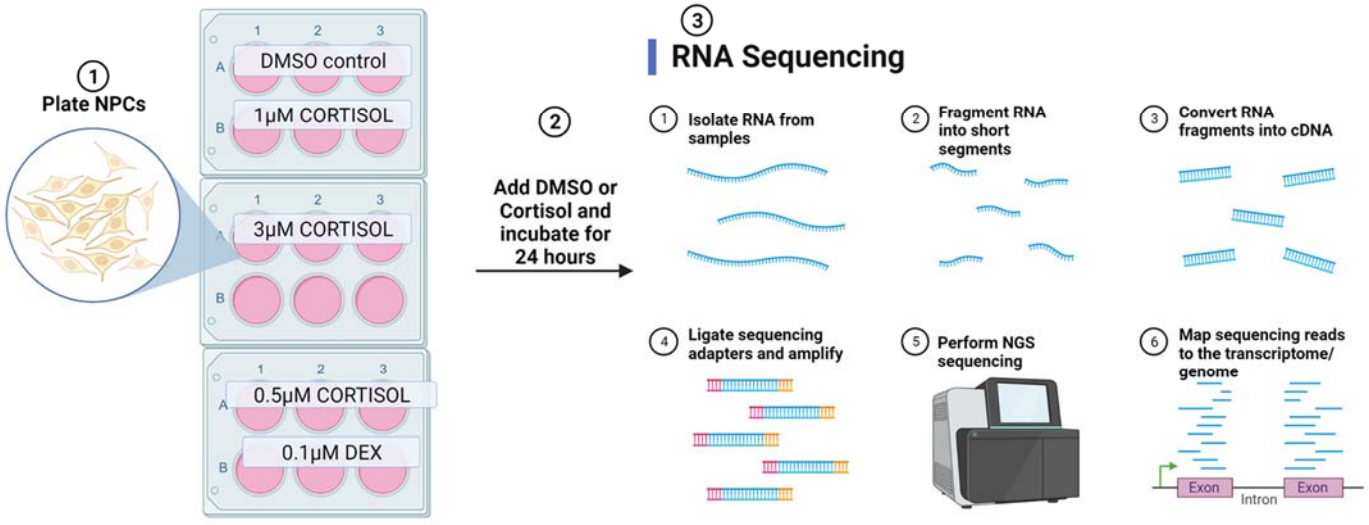

Figure 3.27: Experimental design for RNA sequencing

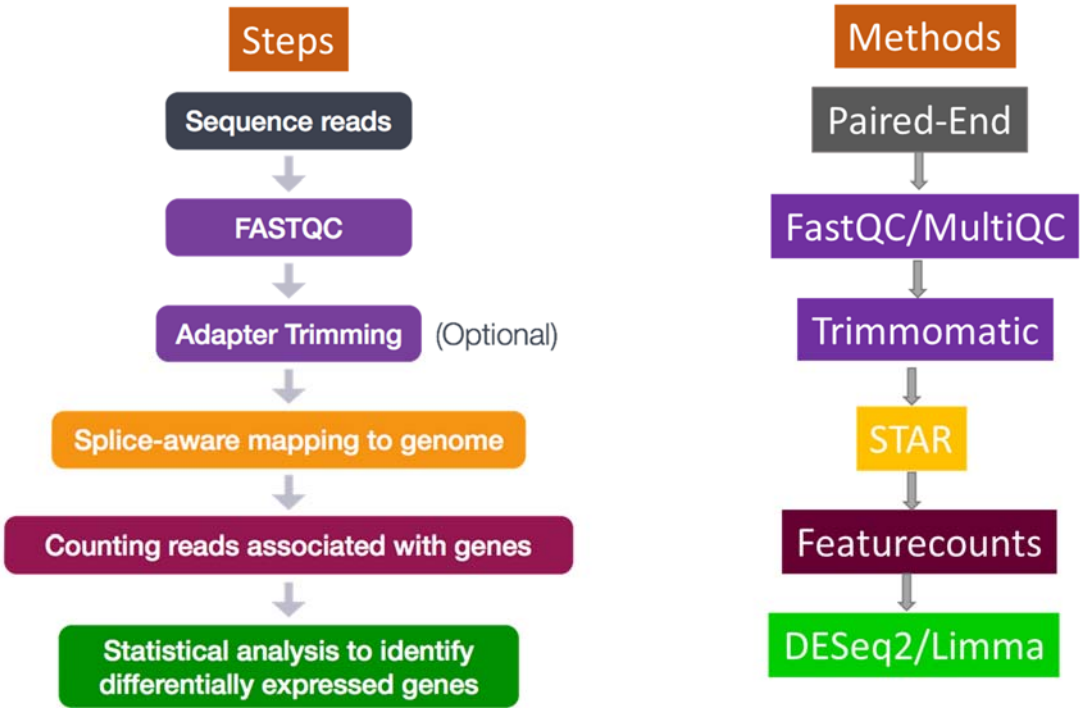

Figure 3.28: Steps used to perform RNA sequencing analysis.

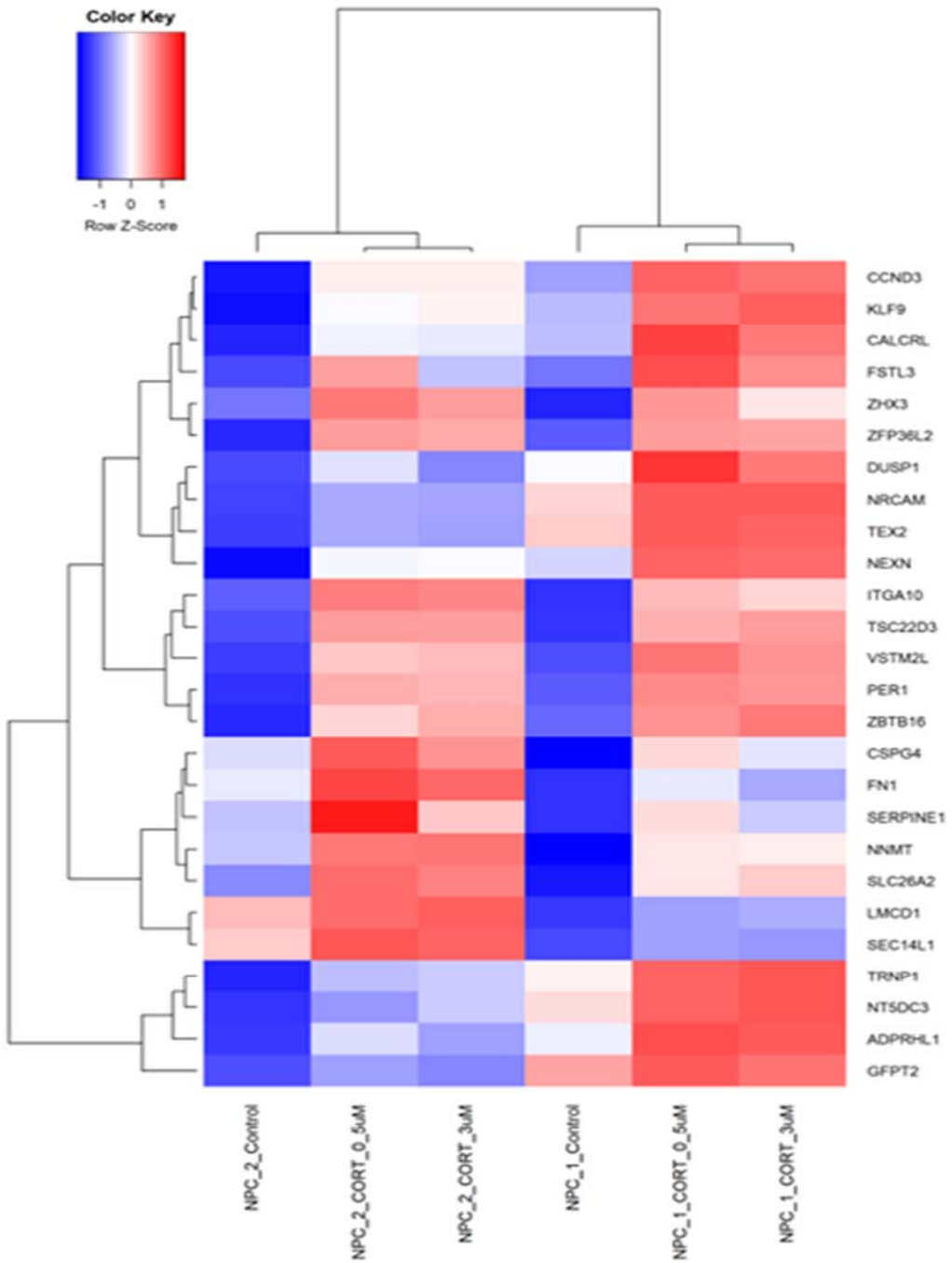

Figure 3.29: Heatmap of Differentially expressed genes in Controls, Cortisol 0.5µM & Cortisol 3µM treated NPCs.

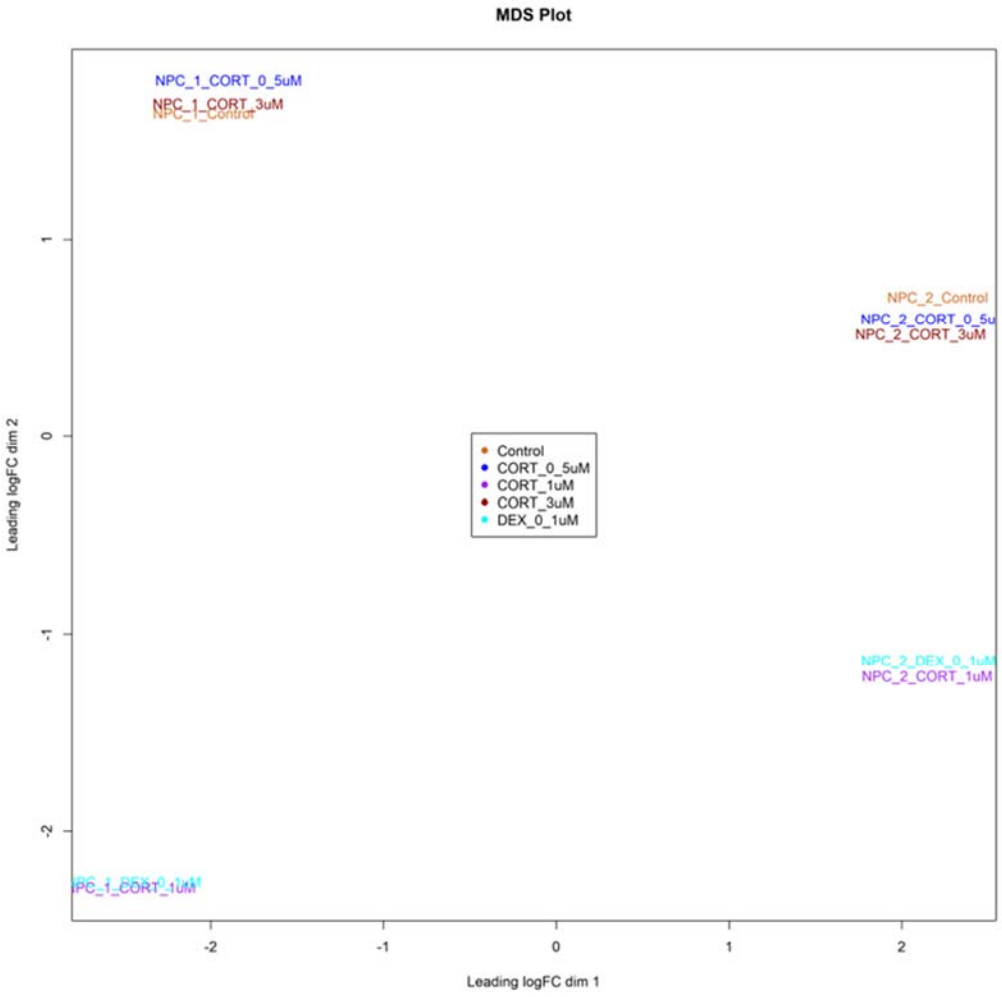

Figure 3.30 : PCA analysis of NPC gene expression after batch effect adjustment

Table 3.3: Differentially expressed genes in NPCs after 24-hour cortisol 0.5μM and 3μM treatment.

geneID	**logCPM**	**pvalue**	**FDR**	**FoldChange**	**cortisol Treatment**
ZBTB16	6.35776	3.28E-08	0.000453	2.426362237	0.5μM and 3 μM
TSC22D3	4.7428571	6.38E-08	0.000453	3.239979724	0.5μM and 3 μM
PER1	6.0322915	8.89E-08	0.000453	2.250017672	0.5μM and 3 μM
ITGA10	3.7856105	7.35E-07	0.002306	3.065800643	0.5μM and 3 μM
TRNP1	4.6656573	7.55E-07	0.002306	2.268378748	0.5μM and 3 μM
SLC26A2	6.9585481	1.1E-06	0.002563	1.782820241	0.5μM and 3 μM
VSTM2L	4.0166097	1.17E-06	0.002563	3.392103669	0.5μM and 3 μM
NT5DC3	6.4203899	1.84E-06	0.003522	1.948853331	0.5μM and 3 μM
NEXN	5.4158629	2.87E-06	0.00488	1.945097584	0.5μM and 3 μM
PDZD2	5.2626703	6.29E-06	0.009604	1.70080752	3μM
IL11	4.7815996	9.31E-06	0.012736	-2.121361318	3μM
SYNJ2	6.8991771	1E-05	0.012736	-1.825750005	3μM
CCND3	5.8685631	1.15E-05	0.012998	1.526644368	0.5μM and 3 μM
KLF9	5.8628408	1.19E-05	0.012998	1.536463751	0.5μM and 3 μM
NNMT	6.8807732	1.31E-05	0.013344	1.832789299	0.5μM and 3 μM
TEX2	7.8290764	1.45E-05	0.013512	1.423796868	0.5μM and 3 μM
ZFP36L2	6.9078708	1.5E-05	0.013512	1.460050415	0.5μM and 3 μM
SAMD4A	7.9885595	1.62E-05	0.013733	1.429529511	3μM
LMCD1	7.8632989	1.94E-05	0.015634	1.480477658	0.5μM and 3 μM
FOXO1	5.3720024	3.18E-05	0.023863	1.582886123	3μM
F2RL2	2.7303058	3.28E-05	0.023863	-2.497807016	3μM
CALCRL	6.4729394	3.52E-05	0.024178	1.436867143	0.5μM and 3 μM
FOSL1	6.3145228	3.64E-05	0.024178	-1.530601654	3μM
SH3BP5	7.1896317	3.98E-05	0.025355	-1.36617854	3μM
GFPT2	6.0115204	4.23E-05	0.025418	1.459086856	0.5μM and 3 μM
SIPA1L2	7.7332063	4.33E-05	0.025418	1.355615316	3μM

PDXK	6.5553071	5.94E-05	0.033243	1.376448331	3µM
TENM4	4.887698	6.24E-05	0.033243	1.533518897	3µM
GRAMD2B	5.5389317	6.74E-05	0.033243	1.476778593	3µM
ADPRHL1	3.8776813	6.8E-05	0.033243	2.340674087	3µM
SEC14L1	8.2904396	6.82E-05	0.033243	1.396091922	0.5µM and 3 µM
SLC4A7	8.1934693	6.96E-05	0.033243	-1.566613446	3µM
IFI44L	5.8326885	7.71E-05	0.035703	-1.399508872	3µM
CHN1	7.893709	8.85E-05	0.03975	1.346749146	3µM
NRCAM	8.8110888	9.49E-05	0.040531	1.326624743	0.5µM and 3 µM
RASSF4	4.8374357	9.55E-05	0.040531	1.620854549	3µM
DSEL	7.1189369	0.000102	0.04116	1.346496065	3µM
POU2F2	3.3198706	0.000102	0.04116	-1.988861693	3µM
ITGB8	7.6340541	0.000107	0.04201	1.544012963	3µM
TMEM150A	4.9405206	0.000118	0.045091	1.435659858	3µM
ZHX3	6.1905642	0.000121	0.045241	1.341425758	0.5µM and 3 µM
SORT1	8.662618	0.00013	0.045569	1.317174923	3µM
PDZRN3	6.3758014	0.000131	0.045569	1.325749541	3µM
ACSL1	6.0252251	0.000139	0.045569	1.571380538	3µM
ATP13A2	7.0086746	0.000143	0.045569	1.578557556	3µM
STIM1	7.0046352	0.000143	0.045569	1.363768494	3µM
USP12	6.4423494	0.000144	0.045569	1.324533359	3µM
UPP1	6.3454599	0.000146	0.045569	-1.64748098	3µM
CNIH3	5.0700884	0.000148	0.045569	-1.414457917	3µM
BCL6	6.3665421	0.000152	0.045569	1.662059012	3µM
FOSL2	7.9740386	0.000152	0.045569	1.348831724	3µM
OMD	1.1732289	0.000161	0.046831	3.699671124	3µM
PCDHGC5	5.859226	0.000164	0.046831	-1.363409033	3µM
JUN	7.6499082	0.000166	0.046831	-1.447623565	3µM
CSPG4	6.7593621	3.36E-05	0.022291	1.533625117	0.5µM
SERPINE1	10.825665	3.27E-06	0.004995	1.909066857	0.5µM

FN1	11.749092	2.52E-05	0.0203	1.494091351	0.5μM
DUSP1	5.3221438	5.79E-05	0.035412	1.580748998	0.5μM
FSTL3	4.7004666	3.21E-05	0.022291	1.890726662	0.5μM

Table 3.4: KEGG Pathway analysis of differentially expressed genes in NPCs after 24-hour cortisol 0.5μM treatment.

	Pathway	Genes
hsa04218	Cellular Senescence	CCND3, SERPINE1, ZFP36L2
hsa04510	Focal adhesion	CCND3, ITGA10, FN1
hsa05165	Human papillomavirus infection	CCND3, ITGA10, FN1
hsa04151	PI3K-Akt signaling pathway	CCND3, ITGA10, FN1

Table 3.5: KEGG Pathway analysis of differentially expressed genes in NPCs after 24-hour cortisol 3μM treatment.

	Pathway	Genes
hsa04510	Focal adhesion	CCND3, JUN, ITGA10, ITGB8
hsa04380	Osteoclast differentiation	FOSL1, JUN, FOSL2
hsa05165	Human papillomavirus infection	CCND3, ITGA10, ITGB8, FOXO1
hsa04218	Cellular senescence	CCND3, FOXO1, ZFP36L2

Table 3.6: GWAS associations of differentially expressed genes in NPCs after cortisol treatment.

Gene	Trait	P-value	PubMed
ZBTB16	Anxious feelings	1.4574e-8	29500382
	Anxious feelings	9.3571e-8	31427789
PER1	Chronotype	7.9263e-12	30696823
	Morning person (binary)	1.5897e-10	30696823
	Chronotype	1.0573e-9	30804565
	Chronotype	1.6884e-9	31427789
	Worry subcluster	3.8632e-8	29942085
FOSL1	Educational attainment	9.4493e-8	30038396
SH3BP5	Temporal horn volume (GEE, adjusted for multivariable)	6.30E-08	17903297
TENM4	Alcohol dependence	3.6172e-12	23089632
	Education - Qualifications	2.1802e-11	31427789
	Intelligence	5.9672e-11	29942086
	Educational attainment	6.7592e-10	30038396
POU2F2	Getting up in morning	5.2589e-12	31427789
	Ease of getting up in the morning	1.2341e-11	30804565
	Number of sleep episodes	2.4419e-9	30952852
ZHX3	Nap during day	7.84E-08	31427789
SORT1	Cognitive performance	1.35E-13	30038396
	Intelligence	3.25E-12	29942086
	Educational attainment	4.6456e-12	30038396
	Fluid intelligence test - Fluid intelligence score	4.4781e-11	31427789
	Verbal-numerical reasoning	3.8053e-10	29844566
	Fluid intelligence score	3.3305e-8	31427789
KLF9	Educational attainment	2.072e-8	30038396

DISCUSSION

In this project, human iPSCs were differentiated to NPCs and the effect of cortisol on NPC function and gene expression was determined. NPCs were differentiated from Human iPSCs, and cell type was confirmed by SOX2, SOX1, PAX6, Nestin expression and loss of undifferentiation marker SSEA-4 by immunofluorescence and qPCR. A novel Nestin isoform that may be present in NPCs but not in iPSCs was identified in this study. Some GC response genes were upregulated after cortisol treatment in NPCs (qPCR). 59 Genes were differentially expressed in cortisol treated NPCs compared to controls (RNA-seq) out of which 9 genes are associated with psychiatric traits based on GWAS studies.

4.1 Cell type confirmation of iPSCs and NPCs

When using marker genes to confirm iPSC and NPC, we detected gene expressions consistent with literature and unexpected differences. Cell type was confirmed using iPSC and NPC marker gene and protein expression by qPCR and immunofluorescence. SSEA4, undifferentiated marker was expressed in iPSC but not in NPCs. This loss of undifferentiation marker SSEA4, suggests that NPCs are differentiated, which was also confirmed in a study that differentiated human ESCs to NPCs [69]. NPCs expressed SOX2, Nestin, SOX1 and PAX6 which was quantified from immunofluorescence and qPCR analyses (Section 3.2).

Quantification of protein expression by IF worked well for SOX2, SOX1, and PAX6, but not for NES. Results from immunofluorescence analysis showed that SOX2, SOX1 and PAX6 are localized in the nucleus whereas Nestin is localized in cytoplasm. The percentage of SOX2, SOX1 and PAX6 expressing NPCs were quantified based on colocalized signals with the nuclear marker DAPI. The quantification of Nestin positive cells was challenging due to the lack of boundaries that could be defined.

Based on literature, iPSC and NPC marker expression were consistent, except for PAX6 and SOX1. Previous studies have reported SOX2, Nestin, PAX6 and SOX1 expression in iPSCs and NPCs. SOX2 and Nestin is expressed in both iPSCs and NPCs by qPCR and

immunofluorescence [70-72]. Flow cytometry and western blot did not detect PAX6 expression in iPSCs. However, PAX6 expression in iPSCs was confirmed by qPCR and immunofluorescence [71-73]. Different methods provided different results regarding the expression of PAX6 in iPSCs. Similarly, SOX1 expression was absent in iPSCs in a previous report [74]. However, in this study SOX1 was expressed in iPSCs (Section 3.2). iPSCs that did not express SOX1 were derived from astrocytes whereas iPSCs used in this study were derived from fibroblasts [74]. The source of iPSCs might impact SOX1 expression. PAX6 and SOX1 are commonly used to identify NPCs, however iPSCs may undergo spontaneous differentiation that can lead to unexpected expression of genes [75]. CNVs (Copy number variants) in iPSCs have also been reported that could affect the differentiation potential [75]. We cannot rule out the contamination of differentiated non-iPSC cells contributing to the detection of PAX6 and SOX1 in our iPSCs.

The LIBD stem cell RNA seq data for iPSC to Neuron differentiation (http://stemcell.libd.org/scb/) showed low expression for SOX1 and PAX6 and high SOX2 expression in iPSCs and increased expression of SOX1, PAX6, similar SOX2 expression in NPCs compared to iPSCs. This is consistent with our qPCR results.

NES expression could not be obtained from LIBD stem cell browser. Similarly SSEA4 expression was also absent in LIBD data. NES was expressed in iPSCs and NPCs in our qPCR and RNA sequencing (Sections 3.2, 3.8). SSEA4 expression was determined using immunofluorescence only in this study (Section 3.2). qPCR based quantification of SSEA4 mRNA expression in iPSCs and NPCs should also be considered.

4.2 Novel Nestin isoforms may be present in NPCs but not in iPSCs

Novel Nestin isoforms may be present in NPCs but not in iPSCs. Surprisingly, one of the primer pairs that was designed to amplify NES, only showed amplification in iPSCs but not in NPCs (Appendix 1 and 2). This primer (NES 1) amplified regions between exon 1 and 2. Currently, only one NES sequence is known to us according to UCSC genome browser. Recent, unpublished data from our collaborators Dr. Pinto and Dr. Gandal labs identified novel short

isoforms of NES in adult and fetal human brain Iso-seq and single cell Iso-sequencing. These isoforms are shown in Appendix Figure 3 and 4. Iso-seq has several advantages. Iso-seq has longer read lengths compared to previous sequencing technologies. Since we can get longer reads, we can sequence full-length transcripts that will allow us to identify novel genes and novel isoforms of known genes [76]. NES isoform differences in NPCs were also identified in RNA sequencing analysis (Appendix Figure 5). This suggests that there may be novel NES isoforms in NPCs. Further comparisons using RNA sequencing data from iPSCs and NPCs could provide information about cell type specific differences of NES isoforms.

Nestin ORFs (open reading frame) were determined using https://www.ncbi.nlm.nih.gov/orffinder/. Full length nestin isoform (known sequence) has a longest open reading frame from 144 (exon 1) to 5009 (exon 4) with 4866 nucleotides and 1621 amino acids. In the absence of exon 1, the shorter Nestin isoform would contain ORF between 1020 (exon 2) to 5009 (exon 4) with 3990 nucleotides and 1329 amino acids. There is a difference of 292 amino acids between this longer and shorter isoforms. There are secondary structure differences between the two protein sequences (for example helical structure), based on the analysis of protein sequences using https://predictprotein.org/. The presence of any conserved domains was analyzed using conserved domain search https://www.ncbi.nlm.nih.gov/Structure/cdd/wrpsb.cgi. Nestin full length protein has filament, smc and smc_prok_B_superfamily domains whereas the shorter form does not contain these domains. These domains seem to be important functional structures for Nestin.

4.3 GC response genes in cortisol treated NPCs

BDNF was one of the GC response genes that was selected for qPCR measurement after cortisol treatment. We screened IPA pathways for Glucocorticoid Receptor regulated genes and genes involved in neuron development and found that three genes (BDNF, POMC and TGFBR2) that are regulated by GR are also involved in neuron development. BDNF is specific to neurons whereas POMC and TGFBR2 are also expressed in other brain cell types in single cell RNA-seq data from Human protein atlas. BDNF is associated with Depression, Anxiety and Bipolar (p-value 10^-7 in GWAS and gda=0.6 disease association score in DisGeNeT) whereas the other

two genes are not significantly associated with psychiatric disorders according to GWAS Atlas and DisGeNeT. cAMP pathway was shared between BDNF and POMC in KEGG pathway analysis. BDNF regulates several processes in neuron development such as proliferation, growth, synaptic plasticity, and LTP [77].The mechanism by which BDNF regulates these processes need to be studied in human cellular models. Stress reduces BDNF expression in animal models of maternal separation [78]. Previous studies have shown that Dexamethasone (GR agonist) decreases BDNF expression in mice, however whether cortisol regulates BDNF and receptor expression during neuron development in human iPSC-neuron differentiation model was not explored before [79]. Variants in BDNF and TrkB (BDNF receptor gene) are associated with psychiatric disorders – anxiety, neuroticism (GWAS atlas). Therefore, BDNF is a key gene that could be regulated by cortisol. However, dexamethasone 0.1μM treatment in NPCs decreased BDNF mRNA expression while cortisol 1μM treatment increased BDNF mRNA expression (Section 3.4). This effect was seen only in one NPC line but not in the other.

There was variation in the response to cortisol among the two NPC lines, which could be explained by genetic factors, length of cortisol exposure and cortisol concentrations. Dexamethasone (activates glucocorticoid receptor) treatment upregulates FKBP5 [80], TSC22D3[81], and ZBTB16 [82] mRNA expression (in brain organoids [83]). Interestingly, FKBP5 mRNA expression was not increased significantly by Dexamethasone and cortisol. ZBTB16 and TSC22D3 mRNA expression were upregulated in cortisol 0.5μM and 3μM treated NPCs (Section 3.4). Comparison of FKBP5 mRNA expression differences between controls and dexamethasone treatment in fibroblasts and iPSC derived neural cells, found a greater increase (670%) in fibroblasts compared to neural cells [84]. This could be due to genetic variations between cell lines, which was not identified in our study. In a population genetic study, SNPs associated with cortisol response in children were identified [85]. Other factors that could contribute to this variation are exposure length and cortisol concentrations. Longer exposure may help us identify more genes, however there is a risk for technical variations due to longer time period for cell maintenance. Moreover, long exposure will not be able to differentiate direct response genes from downstream response genes.

FKBP5 and BDNF methylation is linked to stress and psychiatric disorders. Although, cortisol treatment in NPCs did not affect FKBP5 and BDNF mRNA expression, other relevant regulatory mechanisms could be impacted by cortisol treatment such as DNA methylation. BDNF and FKBP5 methylation are associated with maternal stress and adverse childhood experiences[86, 87]. Furthermore, studies have also suggested the use of FKBP5 and BDNF methylation as biomarkers for cortisol level and psychiatric disorders [88, 89]. DNA methylation of FKBP5 and BDNF could be explored in future study.

4.4 NPC viability measurement

The effect of cortisol on cell viability was determined to confirm that cortisol did not cause cell death. Cortisol did not impact cell viability in NPCs (Section 3.5). In this study only one concentration of cortisol was tested. It is possible that at higher concentrations cortisol may decrease cell viability. The results obtained using MTS and live/stain methods were consistent in showing that cortisol did not have any effect on NPC viability at 3µM concentration.

4.5 NPC proliferation measurements

NPC proliferation response was studied to measure functional effects of cortisol. Ki67 is a suitable measure to quantify proliferation. NPCs did not proliferate significantly after cortisol treatment (Section 3.6). However, there were proliferation related genes that were differentially regulated in RNA seq analysis of cortisol treated NPCs (Discussed in 4.7). Ki67 is specific to actively dividing cells [90]. Ki67 can be detected and quantified easily using immunofluorescence and image analysis.

An alternative approach to Ki67 is the use of EdU quantification to measure proliferation. EdU staining and imaging was established in this study (Section 3.6). EdU is a highly sensitive method for detecting DNA synthesis in proliferating cells. EdU is a thymidine analog that is incorporated into newly synthesized DNA during the S-phase of the cell cycle. This incorporation is facilitated by a copper-catalyzed click reaction between EdU and a fluorescent dye, which allows for direct detection of DNA synthesis using fluorescence microscopy or flow

cytometry [91]. The sensitivity of EdU is much higher than traditional methods such as bromodeoxyuridine (BrdU) incorporation, which requires harsh denaturation of DNA for detection.

4.6 FKBP5 protein expression in NPCs

Previously, we discussed that FKBP5 mRNA expression did not increase after cortisol treatment. Similarly, FKBP5 protein expression did not increase after cortisol treatment in NPCs, which was determined using western blot. According to the human protein atlas database FKBP5 is localized to the nucleoplasm, based on immunostaining in HEK-293 and A-431 cells. Immunofluorescence in cortisol treated cells could be used to measure FKBP5 expression and localization. However, FKBP5 protein expression in NPCs was confirmed using western blot (Section 3.7). Proteins were extracted using mPER Mammalian Protein Extraction Reagent that contains a detergent (proprietary) in 25 mM bicine buffer. mPER extracts both cytoplasmic and nuclear protein from mammalian cells. Therefore, we expect all FKBP5 to be detected in Western blot. Exposure settings were maximized to visualize FKBP5 in immunoblot. Additionally, biotinylated antibodies could be used to detect low abundance proteins, through strong biotin streptavidin interactions.
Substrates (luminol:peroxide) used to visualize blots can be modified. Clarity substrate from BioRad was used in this study. Clarity max substrate (proprietary modifications) could be used to improve the sensitivity of FKBP5 detection with shorter exposure.

4.7 Challenges in RNA sequencing study design and differential gene analysis

RNA sequencing is a widely used technique to analyze the transcriptome in cells. RNA sequencing can be used to quantify gene expression levels, alternative splicing, and fusion transcripts.

Previously the effect of dexamethasone (synthetic GC) on NPC transcriptome in mouse neural cells and iPSC derived brain organoids were determined using RNA-seq [83, 92].There is no

study of transcriptomic changes induced by cortisol on human NPCs. This study is novel since we have explored the role of cortisol in iPSC derived NPCs.

Batch effects can contribute to differential gene expression analysis. iPSC derived NPCs were treated with DMSO, Dexamethasone (0.1μM), cortisol 0.5μM, 1μM or 3μM for 24 hours followed by RNA extraction and sequencing. Dexamethasone (0.1μM) and Cortisol 0.5μM treatments were done on different day, while the other treatments occurred on the same day. Therefore, Dexamethasone (0.1μM) and cortisol 0.5μM treated samples were considered as a separate batch while DMSO, cortisol 0.5μM and 3μM treated samples belong to one batch. Batch effects were corrected using two separate methods ComBat in sva package and removebatcheffects function in Limma. ComBat uses an empirical Bayes method while limma uses two-way ANOVA to correct batch effects. ComBat is a preferred method since it avoids over-correcting and is suitable for small batches. However, since the samples were not evenly distributed amongst the batches and the sample size is small, batch correction methods were not sufficient to correct this effect [93]. If we continued with analyses after ComBat/Limma batch effect correction, we would identify several significantly thousands of significantly regulated gene resulting from an inflated false positive rate. Therefore, we exclude Dexamethasone (0.1μM) and cortisol 0.5μM treated samples from the analyses, and analyzed only one batch of the data.

There are several methods to quantify expression from RNA sequencing result. Paired end sequencing was conducted on cortisol treated NPCs [94]. Using paired end sequencing we can sequence both ends of a fragment. A study that compared expression estimates between single end and paired end sequencing found that short, paired end reads give robust expression estimates that are highly correlated with long single end reads for the same cost [94]. Using featurecounts, expression was quantified after alignment. There are several methods for expression quantification such as RSEM, kallisto, Salmon, cufflinks. These different methods of quantification differ based on the input file requirement (BAM or Fastq), quantification level (Gene or Transcript), confidence levels, strategy to count multi-mapping reads. For example, the major difference between featurecounts and RSEM is that featureCounts discards all multi-

mapping reads, while RSEM uses an expectation-maximization to optimally assign (fractional) counts from multi-mapping reads [95].

Differential expression can be determined using several methods such as limma, edgeR and Deseq2. Differential expression was calculated using edgeR in this study. There are other methods for differential expression analysis such as Deseq2 and limma [96]. EdgeR is suitable for RNA seq analysis, whereas limma is used for both microarrays and RNA seq. The limma, EdgeR and DESeq2 are used for differential analysis but differ in their processes. For example, DESeq2 uses normalization to correct data whereas EdgeR and limma require normalized RNA-seq count data. Statistical tests in EdgeR are based on negative binomial distributions whereas limma uses linear model.

4.8 Altered genes and pathways in transcriptomic response to cortisol in NPCs.

RNA sequencing analysis identified 59 genes that were differentially regulated after cortisol treatment in NPCs. ZBTB16 and TSC22D3 were top differential genes in this analysis. ZBTB16 and TSC22D3 were selected for qPCR studies based on existing literature. Therefore, RNA seq results independently validate the results of qPCR. Similar to protein expression results, FKBP5 was not significantly upregulated in RNA seq studies.

Based on Functional Enrichment analysis using KEGG, Focal adhesion, HPV infection and cellular senescence pathways were shared between exposure to cortisol 0.5μM and 3μM. Although there was no significant change in cell proliferation in functional studies, several genes in cellular senescence pathway were differentially expressed such as CCND3, SERPINE1, FOXO1, ZFP36L2. For example, FOXO1 promotes proliferation in cancer cells and its deficiency promotes neuronal differentiation [97, 98]. We do not see cell proliferation and viability changes in NPC in experiments but observe some related differential gene expression. This could be due to the concentration of cortisol used in the experiments. Viability and Proliferation was measured at 3μM cortisol concentrations. Higher concentrations of cortisol may influence viability and proliferation. Also, differential gene expression may not correlate

with protein levels since translation and post translational modifications can be regulated independently.

Genes associated with anxious feelings, chronotype and educational attainment were differentially regulated after cortisol treatment in NPCs. Psychiatric disorders are complex genetic disorders. Nine genes out of 59 differentially regulated genes were associated with psychiatric traits in GWAS studies according to GWAS atlas data. ZBTB16 and PER1 were associated with anxious feelings and worry. ZBTB16 was also associated with several regions of the brain in brain imaging genetics analysis (white matter and grey matter etc).

PER1 was also associated with chronotype in GWAS atlas. Several studies have explored whether circadian genes are relevant to mood disorders [99]. PER1 is a circadian gene. A recent study identified risk allele in PER1 that is associated with depression and brain white matter characteristics [100].

FOSL1, TENM4, SORT1 and KLF9 were associated with educational attainment and intelligence in GWAS Atlas. In Psychiatric disorders such as Schizophrenia, there is a drop in IQ between ages 13 and 38 years [101]. This suggests that stress may influence genes associated with intelligence and increase the risk for intelligence phenotypes in associated diseases such as schizophrenia. Further evidence is required to understand the link between stress and genes involved in intelligence and psychiatric disorders.

Limitations

While there are several advantages in our experimental design such as using cortisol to model prenatal stress in NPCs which is physiologically relevant compared to synthetic GCs, a few limitations that can be addressed in future experiments have been identified:

- Cells were seeded at a lower density than the density recommended for maintenance. Studying response to cortisol at different cell seeding densities will determine whether cell density affect the outcomes of cell proliferation, differentiation, viability and gene expression in response to cortisol treatments.

- Only one concentration of cortisol was used in this study for viability and proliferation experiments. Higher cortisol concentrations may influence viability and proliferation.
- Study design for RNA sequencing analysis had batch effects. It is best to avoid batch effects if possible or at least have evenly distributed batches.
- Small sample size was an additional factor that limited our statistical analysis in experiments. Due to this, statistical tests are unreliable since there is a low power and low confidence levels on the results as the margin of error is increased. With a small sample size, we cannot ascertain whether the data are normally distributed, therefore nonparametric tests such as Mann Whitney U test would be more suitable for such analysis. Large sample study is needed to replicate findings from this study.

Future Directions

Glucocorticoid receptor specific effects should be determined. Dexamethasone is glucocorticoid receptor agonist, whereas cortisol has high affinity for mineralocorticoid receptor and glucocorticoid receptor. RNA sequencing of NPCs showed expression of glucocorticoid receptor NR3C1 (logCPM=6.7604) and mineralocorticoid receptor NR3C2 (logCPM=5.0495) (Data not shown). Mineralocorticoid receptor protein expression in NPCs should be confirmed by western blot or immunofluorescence. In order to fully understand glucocorticoid receptor mediated gene signatures we should inhibit mineralocorticoid receptor expression (using an inhibitor such as spironolactone) in cortisol treatment studies. RNA sequencing study of cortisol treated NPCs did not fully establish glucocorticoid receptor specific transcription (Section 3.8). The transcriptomic profiles after cortisol treatment should be compared at different stages of neuron development in vitro to understand the difference in response during early and differentiated NPCs.

In addition to RNA sequencing, transcription regulation can be studied. Previous study in a zebrafish model has shown an increase in open chromatin regions in adult blood cells that were treated with cortisol in the embryo stages [102]. Given that ZBTB16 and TSC22D3 are transcription factors that were differentially regulated after cortisol treatment in NPCs (Section 3.8). It would be interesting to examine open chromatin regions in NPCs after cortisol treatment

using approaches such as ATAC-seq followed by quantification of ZBTB16/TSC22D3 protein expression.

The link between cortisol regulated genes and psychiatric disorders can be explored further. Several genes associated with psychiatric traits were identified in this study. SNPs and eQTLs in these genes must be identified in datasets from relevant studies such as fetal brain eQTLs [103]. Associations between cortisol regulated eQTLs and psychiatric disorders need to be established using statistical methods such as Mendelian randomization (MR).

APPENDIX

Supplement Figure 1: Cq Values of NPC marker genes in iPSCs and NPCs

Gene	iPSC (Cq value)	NPC (Cq Value)
SOX2	21.89	26.89
NES-1	28.98	N/A
NES-2	25.84	23.53
NES-3	25.72	23.96
PAX6	25.46	28.75
SOX1	28.52	29.03

Supplement Figure 2: NES Amplification in iPSC and NPC

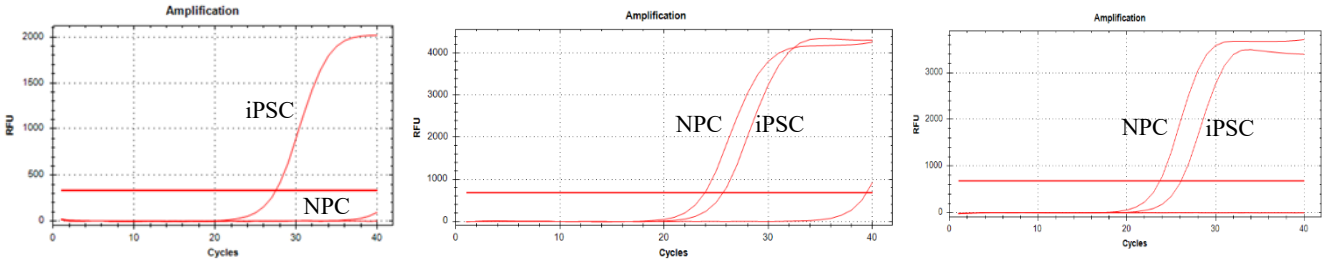

NES 1 NES 2 NES 3

Supplement Figure 3: NES isoforms in adult human brain regions Iso-seq

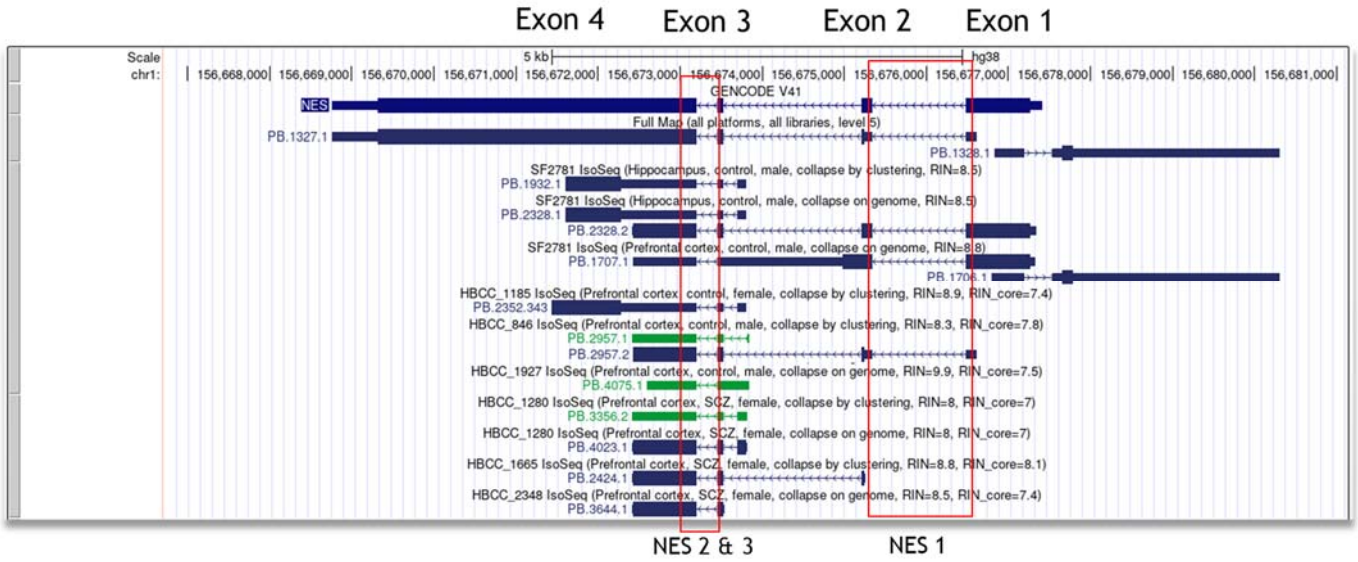

Supplement Figure 4: NES isoforms in fetal human brain single cell Iso-seq

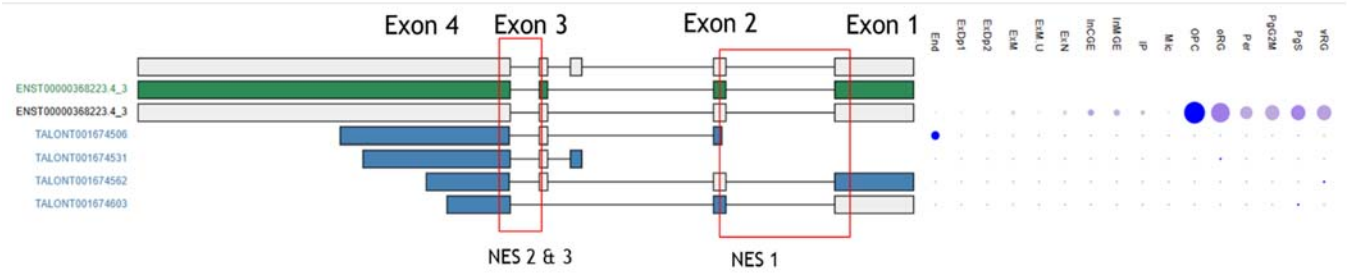

Supplement Figure 5: IGV visualization of NES coverage, splice junctions and alignment from NPC RNA-seq BAM files after STAR alignment

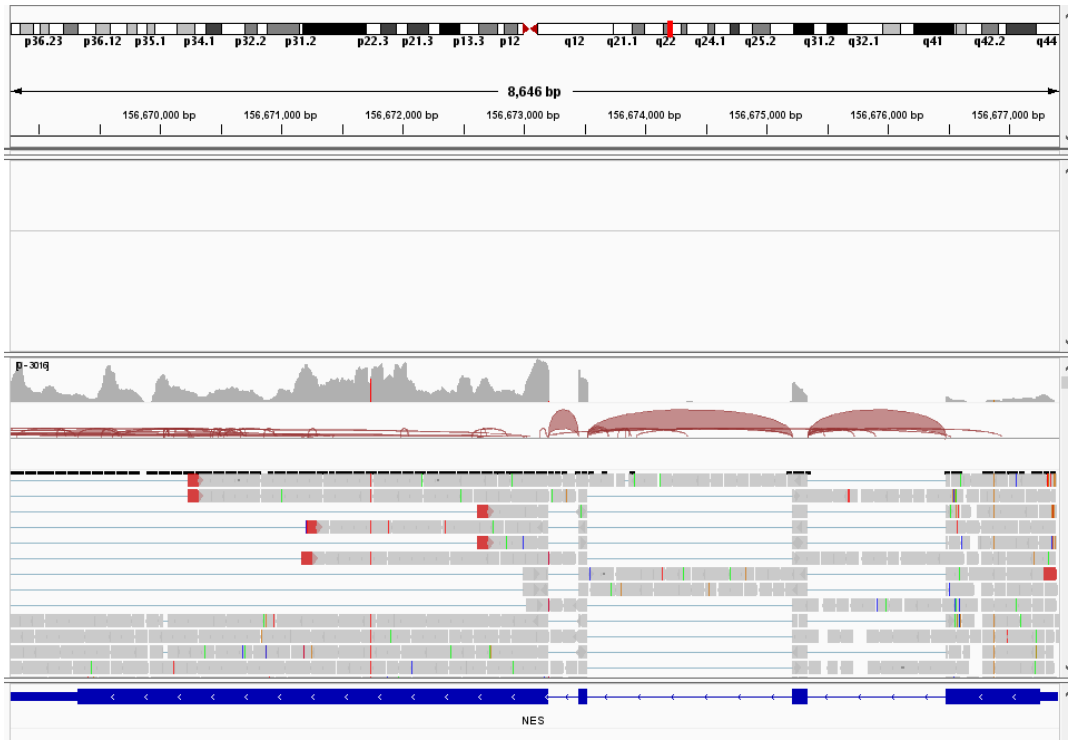

Supplement Figure 6: RNA Quality determined using Agilent Bioanalyzer 2100

Electrophoresis File Run Summary

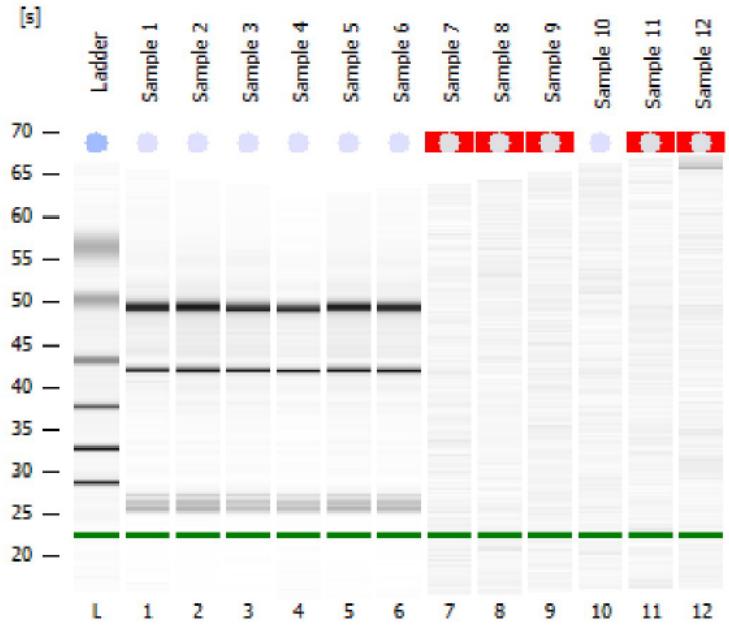

Electropherogram Summary

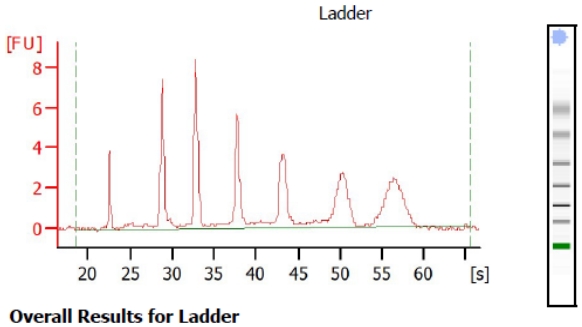

Overall Results for Ladder

RNA Area:	75.7
RNA Concentration:	150 ng/µl
Result Flagging Color:	
Result Flagging Label:	All Other Samples

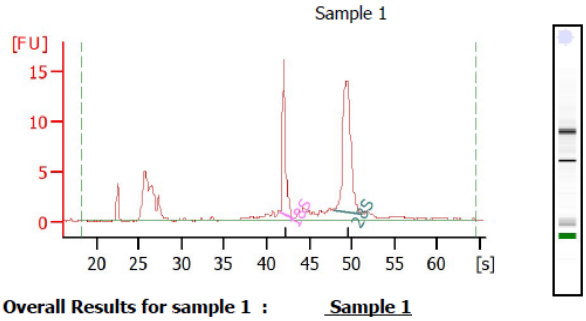

Overall Results for sample 1 : Sample 1

RNA Area:	99.5
RNA Concentration:	197 ng/µl
rRNA Ratio [28s / 18s]:	1.9
RNA Integrity Number (RIN):	9.3 (B.02.09)
Result Flagging Color:	
Result Flagging Label:	RIN: 9.30

Fragment table for sample 1 : Sample 1

Name	Start Time [s]	End Time [s]	Area	% of total Area
18S	41.63	43.13	16.1	16.2
28S	47.95	51.19	29.9	30.0

Supplement Figure 7: FastQC Quality metrics of RNA sequencing Fastq files.

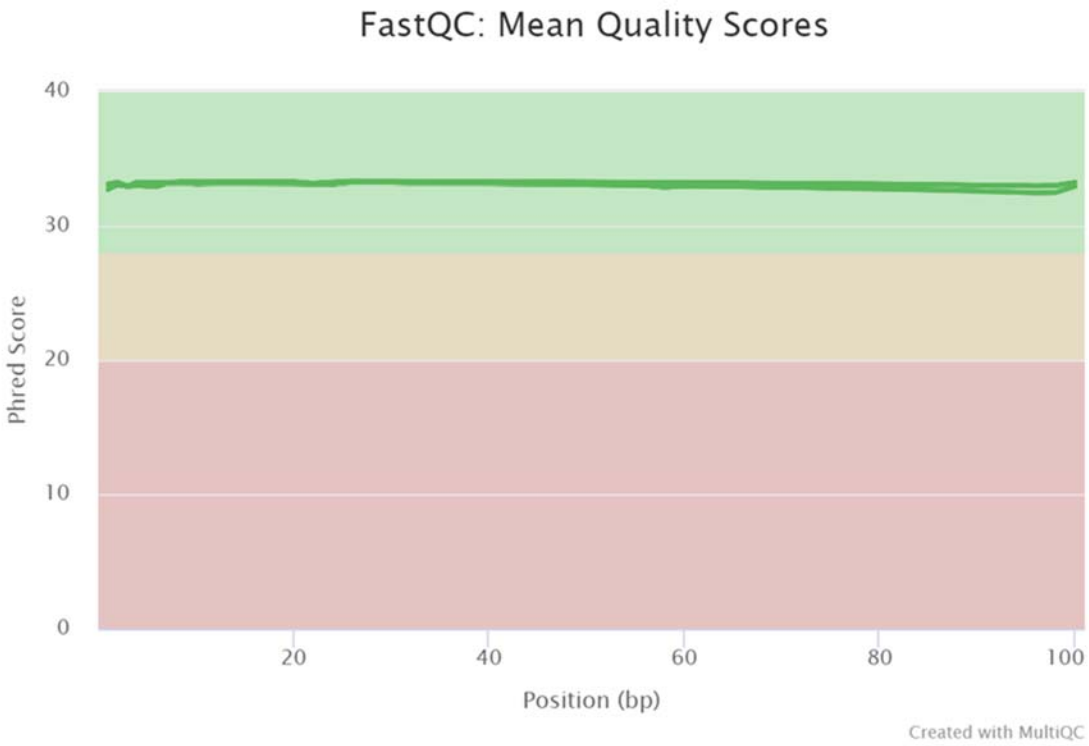

Supplement Table 1: List of Primers

Gene	Forward Primer	Reverse Primer
GAPDH	TGGCCTTCCGTGTCCCCACTGCC	GGGGCCCTCCGACGCCTGCT
C1orf43	CGTACCTCTGAGATCCATTTC	CGTACTAGTGTTTCGCAGATCC
SOX2	AGGATAAGTACACGCTGCCC	TAACTGTCCATGCGCTGGTT
NES 1	GCGTTGGAACAGAGGTTGGA	GAGCGATCTGGCTCTGTAGG
NES 2 (NES)	TCAGCTTTCAGGACCCCAAG	AGGACTGGGAGCAAAGATCC
NES 3	CTCAGCTTTCAGGACCCC	TGGGAGCAAAGATCCAAGAC
PAX6	TAAGGATGTTGAACGGGCAG	GGAGTTGGTATTCTCTCCCCC
SOX1	GCTGACACCAGACTTGGGTT	CCTCTCGCCTCGTTTTGACT
FKBP5	TCCCTCGAATGCAACTC	CAGGTGGATTTCTACTGTTG
ZBTB16	AAGCGGTTCCTGGATAG	CATGTCAGTGCCAGTATG
	GACCCATACTGGCACTG	CTCACTGCAGATGTAGC
TSC22D3	AACACCGAAATGTATCAGACCC	CCGGAGGCACTGTTGTC
	GAGGTGGCGGTCTACCAG	GCTCCGGAGGCACTGTTG
BDNF	GTTTGTGTGGACCCCGAG	GTTTGCTTCTTTCATGGGGG
	GTGAGGTTTGTGTGGACCC	CAGCCTTCATGCAACCAAAG

Supplement Table 2: List of antibodies used.

Antibody	Target Species	Host Species	Type of Marker	Clonality	Company	Catalog No	Concentration	Application
Anti-SSEA4	Human, Mouse, Rabbit	Mouse	iPSC	Monoclonal	Novus	NBP2-26644AF594	1:200	Immunofluorescence
Anti-SOX2	Mouse, Rat, Human	Rabbit	iPSC/NPC	Polyclonal	Abcam	ab97959	1:200	Immunofluorescence
Anti-Nestin	Human	Mouse	NPC	Monoclonal	Santa Cruz	Sc-23927	1:200	Immunofluorescence
Anti-PAX6	Mouse, Rat, Human	Rabbit	NPC	Polyclonal	Biolegend	901301	1:200	Immunofluorescence
Anti-SOX1	Mouse, Rat, Human	Goat	NPC	Polyclonal	R&D	AF3369	1:200	Immunofluorescence
Anti-MAP2	Mouse, Rat and human	Mouse	Neuron	Monoclonal	Synaptic Systems	188 011	1:200	Immunofluorescence
Anti-NeuN	Mouse, Rat, Human	Rabbit	Neuron	Polyclonal	Abcam	ab104225	1:200	Immunofluorescence
Anti-Ki67	Mouse, Human	Rabbit	Proliferation	Polyclonal	Abcam	ab15580	1:500	Immunofluorescence
Anti-GAPDH	Human, Mouse, Rat	Rabbit	Loading Control	Monoclonal	Cell Signaling	2118	1:1000	Western Blot
Anti-FKBP5	Human, Mouse	Rabbit	Cofactor for Glucocorticoid Receptor	Polyclonal	Cell Signaling	8245	1:1000	Western Blot
Rabbit			Secondary Antibody		Abcam	ab150077	1:200	Immunofluorescence
Rabbit			Secondary Antibody		Cell Signaling	7074	1:1000	Western Blot
Mouse			Secondary Antibody		Abcam	ab150107	1:200	Immunofluorescence
Goat			Secondary Antibody		R&D	NL002	1:200	Immunofluorescence

Supplement Table 3: List of iPSC and NPC lines

Clone ID	Sex	Cell type	Age	Disease	Company
5913	M	iPSC	26	Healthy	RUCDR Infinite Biologics
70901	M	NPC	30	Healthy	Stem Cell

REFERENCES

1. Arias, D., S. Saxena, and S. Verguet, *Quantifying the global burden of mental disorders and their economic value.* EClinicalMedicine, 2022. **54**: p. 101675.
2. Collaborators, G.B.D.M.D., *Global, regional, and national burden of 12 mental disorders in 204 countries and territories, 1990-2019: a systematic analysis for the Global Burden of Disease Study 2019.* Lancet Psychiatry, 2022. **9**(2): p. 137-150.
3. Erskine, H.E., et al., *A heavy burden on young minds: the global burden of mental and substance use disorders in children and youth.* Psychol Med, 2015. **45**(7): p. 1551-63.
4. Alachkar, A., et al., *The hidden link between circadian entropy and mental health disorders.* Transl Psychiatry, 2022. **12**(1): p. 281.
5. Gomes, F.V. and A.A. Grace, *Adolescent Stress as a Driving Factor for Schizophrenia Development-A Basic Science Perspective.* Schizophr Bull, 2017. **43**(3): p. 486-489.
6. Hassanzadeh, A., et al., *Association of Stressful Life Events with Psychological Problems: A Large-Scale Community-Based Study Using Grouped Outcomes Latent Factor Regression with Latent Predictors.* Comput Math Methods Med, 2017. **2017**: p. 3457103.
7. Li, M. and L. Wang, *The Associations of Psychological Stress with Depressive and Anxiety Symptoms among Chinese Bladder and Renal Cancer Patients: The Mediating Role of Resilience.* PLoS One, 2016. **11**(4): p. e0154729.
8. Tafet, G.E. and C.B. Nemeroff, *The Links Between Stress and Depression: Psychoneuroendocrinological, Genetic, and Environmental Interactions.* J Neuropsychiatry Clin Neurosci, 2016. **28**(2): p. 77-88.
9. Bennett, H.A., et al., *Prevalence of depression during pregnancy: systematic review.* Obstet Gynecol, 2004. **103**(4): p. 698-709.
10. Sausenthaler, S.e.a., *Stress-Related Maternal Factors During Pregnancy in Relation to Childhood Eczema: Results From the LISA Study.* J Investig Allergol Clin Immunol 2009. **19**(6): p. 7.
11. Pantha, S., *Prevalence of Stress among Pregnant Women Attending Antenatal Care in a Tertiary Maternity Hospital in Kathmandu.* Journal of Women's Health Care, 2014. **03**(05).

12. Saroj Nimkarn, M.I.N., *Prenatal diagnosis and treatment of congenital adrenal hyperplasia owing to 21-hydroxylase deficiency.* Nat Clin Pract Endocrinol Metab, 2007. **3**(5): p. 8.
13. Basirat, Z., et al., *Impact of dexamethasone on pregnancy outcome in PCOs women candidate for IVF/ICSI, a single-blind randomized clinical trial study.* Middle East Fertility Society Journal, 2016. **21**(3): p. 184-188.
14. Athavale, A., T. Athavale, and D.M. Roberts, *Antiemetic drugs: what to prescribe and when.* Aust Prescr, 2020. **43**(2): p. 49-56.
15. Glover, V. and J. Hill, *Sex differences in the programming effects of prenatal stress on psychopathology and stress responses: an evolutionary perspective.* Physiol Behav, 2012. **106**(1873-507X (Electronic)): p. 5.
16. Barker, D.J., *The fetal and infant origins of adult disease.* BMJ: British Medical Journal,, 1990. **301(6761)**(1111).
17. Benediktsson, R., et al., *Placental 11 beta-hydroxysteroid dehydrogenase: a key regulator of fetal glucocorticoid exposure.* Clin Endocrinol (Oxf). , 1997. **46**(0300-0664 (Print)).
18. Mairesse, J., et al., *Maternal stress alters endocrine function of the feto-placental unit in rats.* Am J Physiol Endocrinol Metab, 2007. **292**(6): p. E1526-33.
19. Xu, D., et al., *Dexamethasone induces fetal developmental toxicity through affecting the placental glucocorticoid barrier and depressing fetal adrenal function.* Environ Toxicol Pharmacol., 2011. **32**(1872-7077 (Electronic)).
20. Pearson, R.M., et al., *Maternal depression during pregnancy and the postnatal period: risks and possible mechanisms for offspring depression at age 18 years.* JAMA Psychiatry, 2013. **70**(12): p. 1312-9.
21. Plant, D.T., et al., *Maternal depression during pregnancy and offspring depression in adulthood: role of child maltreatment.* Br J Psychiatry, 2015. **207**(3): p. 213-20.
22. Capron, L.E., et al., *Associations of maternal and paternal antenatal mood with offspring anxiety disorder at age 18 years.* J Affect Disord, 2015. **187**: p. 20-6.
23. Winsper, C., D. Wolke, and T. Lereya, *Prospective associations between prenatal adversities and borderline personality disorder at 11-12 years.* Psychol Med, 2015. **45**(5): p. 1025-37.

24. Li, J., et al., *Attention-deficit/hyperactivity disorder in the offspring following prenatal maternal bereavement: a nationwide follow-up study in Denmark.* Eur Child Adolesc Psychiatry, 2010. **19**(10): p. 747-53.
25. Class, Q.A., et al., *Offspring psychopathology following preconception, prenatal and postnatal maternal bereavement stress.* Psychol Med, 2014. **44**(1): p. 71-84.
26. Buss, C., et al., *Maternal cortisol over the course of pregnancy and subsequent child amygdala and hippocampus volumes and affective problems.* Proc Natl Acad Sci U S A, 2012. **109**(20): p. E1312-9.
27. Ronald, A., C.E. Pennell, and A.J. Whitehouse, *Prenatal Maternal Stress Associated with ADHD and Autistic Traits in early Childhood.* Front Psychol, 2010. **1**: p. 223.
28. Kingsbury, M., et al., *Stressful Life Events During Pregnancy and Offspring Depression: Evidence From a Prospective Cohort Study.* J Am Acad Child Adolesc Psychiatry, 2016. **55**(8): p. 709-716 e2.
29. Rijlaarsdam, J., et al., *Prenatal unhealthy diet, insulin-like growth factor 2 gene (IGF2) methylation, and attention deficit hyperactivity disorder symptoms in youth with early-onset conduct problems.* J Child Psychol Psychiatry, 2017. **58**(1): p. 19-27.
30. Antonow-Schlorke, I., et al., *Glucocorticoid exposure at the dose used clinically alters cytoskeletal proteins and presynaptic terminals in the fetal baboon brain.* J Physiol, 2003. **547**(Pt 1): p. 117-23.
31. Noorlander, C.W., et al., *Antenatal glucocorticoid treatment affects hippocampal development in mice.* PLoS One, 2014. **9**(1): p. e85671.
32. Converse, A.K., et al., *Prenatal stress induces increased striatal dopamine transporter binding in adult nonhuman primates.* Biol Psychiatry, 2013. **74**(7): p. 502-10.
33. Coe, C.L., G.R. Lulbach, and M.L. Schneider, *Prenatal disturbance alters the size of the corpus callosum in young monkeys.* Dev Psychobiol, 2002. **41**(2): p. 178-85.
34. Coe, C.L., et al., *Prenatal stress diminishes neurogenesis in the dentate gyrus of juvenile rhesus monkeys.* Biol Psychiatry, 2003. **54**(10): p. 1025-34.
35. Lucassen, P.J., et al., *Prenatal stress reduces postnatal neurogenesis in rats selectively bred for high, but not low, anxiety: possible key role of placental 11beta-hydroxysteroid dehydrogenase type 2.* Eur J Neurosci, 2009. **29**(1): p. 97-103.

36. Egeland, M., P.A. Zunszain, and C.M. Pariante, *Molecular mechanisms in the regulation of adult neurogenesis during stress.* Nat Rev Neurosci, 2015. **16**(4): p. 189-200.
37. Anacker, C., et al., *Glucocorticoid-related molecular signaling pathways regulating hippocampal neurogenesis.* Neuropsychopharmacology, 2013. **38**(5): p. 872-83.
38. Nurnberg, E., et al., *Basal glucocorticoid receptor activation induces proliferation and inhibits neuronal differentiation of human induced pluripotent stem cell-derived neuronal precursor cells.* J Steroid Biochem Mol Biol, 2018. **182**: p. 119-126.
39. Ninomiya, E.a.a., *Glucocorticoids promote neural progenitor cell proliferation derived from human induced pluripotent stem cells.* Springer Plus, 2014. **3**(527): p. 8.
40. Davis, E.P., et al., *Fetal glucocorticoid exposure is associated with preadolescent brain development.* Biol Psychiatry, 2013. **74**(9): p. 647-55.
41. Moog, N.K., et al., *Intergenerational Effect of Maternal Exposure to Childhood Maltreatment on Newborn Brain Anatomy.* Biol Psychiatry, 2018. **83**(2): p. 120-127.
42. Davis, E.P., et al., *Prenatal Maternal Stress, Child Cortical Thickness, and Adolescent Depressive Symptoms.* Child Dev, 2020. **91**(2): p. e432-e450.
43. *<endo2705 (1).pdf>.*
44. Fletcher, A.J., et al., *Antenatal glucocorticoids reset the level of baseline and hypoxemia-induced pituitary-adrenal activity in the sheep fetus during late gestation.* (0193-1849 (Print)).
45. Davis, E.P., F. Waffarn, and C.A. Sandman, *Prenatal treatment with glucocorticoids sensitizes the hpa axis response to stress among full-term infants.* Dev Psychobiol, 2011. **53**(2): p. 175-83.
46. McGowan, P.O. and S.G. Matthews, *Prenatal Stress, Glucocorticoids, and Developmental Programming of the Stress Response.* Endocrinology, 2018. **159**(1): p. 69-82.
47. Howerton, C.L. and T.L. Bale, *Targeted placental deletion of OGT recapitulates the prenatal stress phenotype including hypothalamic mitochondrial dysfunction.* Proc Natl Acad Sci U S A, 2014. **111**(26): p. 9639-44.
48. Howerton, C.L., et al., *O-GlcNAc transferase (OGT) as a placental biomarker of maternal stress and reprogramming of CNS gene transcription in development.* Proc Natl Acad Sci U S A, 2013. **110**(13): p. 5169-74.

49. Shearer, F.J.G., C.S. Wyrwoll, and M.C. Holmes, *The Role of 11beta-Hydroxy Steroid Dehydrogenase Type 2 in Glucocorticoid Programming of Affective and Cognitive Behaviours.* Neuroendocrinology, 2019. **109**(3): p. 257-265.
50. Stirrat, L.I., et al., *Transfer and Metabolism of Cortisol by the Isolated Perfused Human Placenta.* J Clin Endocrinol Metab, 2018. **103**(2): p. 640-648.
51. Gross, M., et al., *Placental glucocorticoid receptor and 11beta-hydroxysteroid dehydrogenase-2 recruitment indicates impact of prenatal adversity upon postnatal development in mice.* Stress, 2018. **21**(6): p. 474-483.
52. O'Donnell, K.J., et al., *Maternal prenatal anxiety and downregulation of placental 11β-HSD2.* Psychoneuroendocrinology, 2012. **37**(1873-3360 (Electronic)).
53. Glover, V., et al., *Association between maternal and amniotic fluid cortisol is moderated by maternal anxiety.* Psychoneuroendocrinology, 2009. **34**(0306-4530 (Print)).
54. Marsit, C.J., et al., *Placental 11-beta hydroxysteroid dehydrogenase methylation is associated with newborn growth and a measure of neurobehavioral outcome.* PLoS One, 2012. **7**(3): p. e33794.
55. Khalife, N., et al., *Prenatal glucocorticoid treatment and later mental health in children and adolescents.* PLoS One, 2013. **8**(11): p. e81394.
56. Sandman, C.A., et al., *Fetal exposure to maternal depressive symptoms is associated with cortical thickness in late childhood.* Biol Psychiatry, 2015. **77**(4): p. 324-34.
57. Sharp, H., et al., *Frequency of infant stroking reported by mothers moderates the effect of prenatal depression on infant behavioural and physiological outcomes.* PLoS One, 2012. **7**(10): p. e45446.
58. Nugent, B.M., et al., *Placental H3K27me3 establishes female resilience to prenatal insults.* Nat Commun, 2018. **9**(1): p. 2555.
59. Provencal, N., et al., *Glucocorticoid exposure during hippocampal neurogenesis primes future stress response by inducing changes in DNA methylation.* Proc Natl Acad Sci U S A, 2020. **117**(38): p. 23280-23285.
60. Moisiadis, V.G., et al., *Prenatal Glucocorticoid Exposure Modifies Endocrine Function and Behaviour for 3 Generations Following Maternal and Paternal Transmission.* Sci Rep, 2017. **7**(1): p. 11814.

61. Weinstock, M., *Prenatal stressors in rodents: Effects on behavior.* Neurobiol Stress, 2017. **6**: p. 3-13.
62. Stein, J.L., et al., *A quantitative framework to evaluate modeling of cortical development by neural stem cells.* Neuron, 2014. **83**(1): p. 69-86.
63. Brennand, K., et al., *Phenotypic differences in hiPSC NPCs derived from patients with schizophrenia.* Mol Psychiatry, 2015. **20**(3): p. 361-8.
64. Ziller, M.J., et al., *Dissecting neural differentiation regulatory networks through epigenetic footprinting.* Nature, 2015. **518**(7539): p. 355-359.
65. Edri, R., et al., *Analysing human neural stem cell ontogeny by consecutive isolation of Notch active neural progenitors.* Nat Commun, 2015. **6**: p. 6500.
66. Hirabayashi, Y. and Y. Gotoh, *Epigenetic control of neural precursor cell fate during development.* Nat Rev Neurosci, 2010. **11**(6): p. 377-88.
67. Drexler, H.G.U., C.C, *Mycoplasma contamination of cell cultures: Incidence, sources, effects, detection, elimination, prevention.* Cytotechnology, 2002. **39**: p. 15.
68. Murphy, B.E.P., *Cortisol and Cortisone in human fetal development.* Journal of Steroid Biochemistry 1979. **11**: p. 4.
69. Noisa, P., et al., *Identification and characterisation of the early differentiating cells in neural differentiation of human embryonic stem cells.* PLoS One, 2012. **7**(5): p. e37129.
70. Sundberg, M., et al., *Markers of pluripotency and differentiation in human neural precursor cells derived from embryonic stem cells and CNS tissue.* Cell Transplant, 2011. **20**(2): p. 177-91.
71. Hofrichter, M., et al., *Comparative performance analysis of human iPSC-derived and primary neural progenitor cells (NPC) grown as neurospheres in vitro.* Stem Cell Res, 2017. **25**: p. 72-82.
72. Kim, Y.M., et al., *Effects of mechanical stimulation on the reprogramming of somatic cells into human-induced pluripotent stem cells.* Stem Cell Res Ther, 2017. **8**(1): p. 139.
73. Hu, B.Y., et al., *Neural differentiation of human induced pluripotent stem cells follows developmental principles but with variable potency.* Proc Natl Acad Sci U S A, 2010. **107**(9): p. 4335-40.
74. Nakajima-Koyama, M., et al., *Induction of Pluripotency in Astrocytes through a Neural Stem Cell-like State.* J Biol Chem, 2015. **290**(52): p. 31173-88.

75. Yamamoto, T., et al., *Improving the differentiation potential of pluripotent stem cells by optimizing culture conditions.* Sci Rep, 2022. **12**(1): p. 14147.
76. Rhoads, A. and K.F. Au, *PacBio Sequencing and Its Applications.* Genomics Proteomics Bioinformatics, 2015. **13**(5): p. 278-89.
77. Miranda, M., et al., *Brain-Derived Neurotrophic Factor: A Key Molecule for Memory in the Healthy and the Pathological Brain.* Front Cell Neurosci, 2019. **13**: p. 363.
78. Daskalakis, N.P., et al., *Early Life Stress Effects on Glucocorticoid-BDNF Interplay in the Hippocampus.* Front Mol Neurosci, 2015. **8**: p. 68.
79. Chen, H., M. Lombes, and D. Le Menuet, *Glucocorticoid receptor represses brain-derived neurotrophic factor expression in neuron-like cells.* Mol Brain, 2017. **10**(1): p. 12.
80. Menke, A., et al., *Dexamethasone stimulated gene expression in peripheral blood is a sensitive marker for glucocorticoid receptor resistance in depressed patients.* Neuropsychopharmacology, 2012. **37**(6): p. 1455-64.
81. Francesca D'Adamio, O.Z., Rosalba Moraca, Emira Ayroldi, Stefano Bruscoli, Andrea Bartoli, Lorenza Cannarile, Graziella Migliorati, and Carlo Riccardi, *A New Dexamethasone-Induced Gene of the Leucine Zipper Family Protects T Lymphocytes from TCR/CD3-Activated Cell Death.* Immunity, 1997. **7**: p. 10.
82. Kathirvel, K., et al., *Short and long-term effect of dexamethasone on the transcriptome profile of primary human trabecular meshwork cells in vitro.* Sci Rep, 2022. **12**(1): p. 8299.
83. Cruceanu, C., et al., *Cell-Type-Specific Impact of Glucocorticoid Receptor Activation on the Developing Brain: A Cerebral Organoid Study.* Am J Psychiatry, 2021: p. appiajp202121010095.
84. Lieberman, R., et al., *Examining FKBP5 mRNA expression in human iPSC-derived neural cells.* Psychiatry Res, 2017. **247**: p. 172-181.
85. Ersig, A.L., et al., *Genetic Variants and the Cortisol Response in Children: An Exploratory Study.* Biol Res Nurs, 2019. **21**(2): p. 157-165.
86. Kertes, D.A., et al., *BNDF methylation in mothers and newborns is associated with maternal exposure to war trauma.* Clin Epigenetics, 2017. **9**: p. 68.

87. Misiak, B., et al., *Adverse Childhood Experiences and Methylation of the FKBP5 Gene in Patients with Psychotic Disorders.* J Clin Med, 2020. **9**(12).
88. Winkler, B.K., et al., *FKBP5 methylation as a possible marker for cortisol state and transient cortisol exposure in healthy human subjects.* (1750-192X (Electronic)).
89. Zheleznyakova, G.Y., H. Cao, and H.B. Schioth, *BDNF DNA methylation changes as a biomarker of psychiatric disorders: literature review and open access database analysis.* Behav Brain Funct, 2016. **12**(1): p. 17.
90. Gerdes J Fau - Schwab, U., et al., *Production of a mouse monoclonal antibody reactive with a human nuclear antigen associated with cell proliferation.* (0020-7136 (Print)).
91. Mitchison, A.S.a.T.J., *A chemical method for fast and sensitive detection of DNA synthesis in vivo.* PNAS, 2008. **105**(7): p. 6.
92. Frahm, K.A., et al., *Research Resource: The Dexamethasone Transcriptome in Hypothalamic Embryonic Neural Stem Cells.* Mol Endocrinol, 2016. **30**(1): p. 144-54.
93. Nygaard, V., E.A. Rodland, and E. Hovig, *Methods that remove batch effects while retaining group differences may lead to exaggerated confidence in downstream analyses.* Biostatistics, 2016. **17**(1): p. 29-39.
94. Freedman, A.H., J.M. Gaspar, and T.B. Sackton, *Short paired-end reads trump long single-end reads for expression analysis.* BMC Bioinformatics, 2020. **21**(1): p. 149.
95. Deschamps-Francoeur, G., J. Simoneau, and M.S. Scott, *Handling multi-mapped reads in RNA-seq.* Comput Struct Biotechnol J, 2020. **18**: p. 1569-1576.
96. Liu, S., et al., *Three Differential Expression Analysis Methods for RNA Sequencing: limma, EdgeR, DESeq2.* J Vis Exp, 2021(175).
97. Prasad, S.B., et al., *Down Regulation of FOXO1 Promotes Cell Proliferation in Cervical Cancer.* J Cancer, 2014. **5**(8): p. 655-62.
98. Kim, D.Y., et al., *Functional regulation of FoxO1 in neural stem cell differentiation.* Cell Death Differ, 2015. **22**(12): p. 2034-45.
99. *<nihms22412.pdf>.*
100. Zhao, R., et al., *Per1 gene polymorphisms influence the relationship between brain white matter microstructure and depression risk.* Front Psychiatry, 2022. **13**: p. 1022442.

101. Meier, M.H., et al., *Neuropsychological decline in schizophrenia from the premorbid to the postonset period: evidence from a population-representative longitudinal study.* Am J Psychiatry, 2014. **171**(1): p. 91-101.
102. Hartig, E.I., et al., *Chronic cortisol exposure in early development leads to neuroendocrine dysregulation in adulthood.* BMC Res Notes, 2020. **13**(1): p. 366.
103. O'Brien, H.E., et al., *Expression quantitative trait loci in the developing human brain and their enrichment in neuropsychiatric disorders.* Genome Biol, 2018. **19**(1): p. 194.